Optimizing Fuel Efficiency in Intercontinental Passenger Flights: Integrating Air Cargo Palletization and Weight and Balance Problem

A case study for Air France KLM Martinair Cargo

G.A.M. Puttaert

TU Delft

Optimizing Fuel Efficiency in Intercontinental Passenger Flights: Integrating Air Cargo Palletization and Weight and Balance Problem

A case study for Air France KLM Martinair Cargo

by

G.A.M. Puttaert

to obtain the degree of Master of Science
at the Delft University of Technology,
to be defended publicly on Friday July 19, 2024.

Student number:	4686160	
Project duration:	November 29, 2023 - July 19, 2024	
Thesis committee:	Ir. P.C. Roling	TU Delft, Chair
	Dr. A. Bombelli	TU Delft, Supervisor
	Dr. E.J.J Smeur	TU Delft, Examiner
	Dr. F. Delgado	UC Chile, Examiner
	Ir. B.W. van der Wal	KLM, Supervisor

TU Delft

Acknowledgements

Starting November 29th, 2023, I passed through the spinning security door at KLM Cargo for the first time. This marked the beginning of my thesis journey. Little did I know that by July 2024, I would look back on this process as one might reflect on a marathon, with a vocabulary enriched by terms like "Weight and Balance," "Bin Packing," "Heuristic," and "Mean Aerodynamic Chord," or simply "MAC." Each term was similar to a marathon's aid station, pushing me towards the next milestone over the eight months of this sweat. The most critical milestone came at kilometer 32, where a marathon runner often hits the wall. This time, however, the wall did not hit; instead, it integrated the two problems, resulting in positive results for the sustainability and operational effectiveness of the future air cargo industry.

I extend my deepest gratitude to Alessandro Bombelli for his supervision, guidance, and flexibility throughout this process, especially toward the end when planning the graduation date. Alessandro, thank you for your efforts in assembling a committee during the summer and ensuring my entire family could be present at the graduation. It is a date that holds significant meaning for my family and me.

Wouter, thank you for your friendliness and helpfulness from the beginning at KLM. I will remember our laughs and excursions to various divisions and teams throughout KLM, our quick brainstorming sessions when the code wouldn't work, and, of course, the discovery of the "Morph." I look forward to seeing a beautiful slide deck from you soon. I also thank the Performance Management team at KLM for warmly welcoming me since the first day I passed through the spinning security door.

Last but not least, I am profoundly grateful for the support of my family and friends during this marathon. Your encouragement and belief in me were instrumental in completing this process and my time at TU Delft.

G.A.M. Puttaert
Amsterdam, July 2024

Contents

List of Abbreviations **vii**

Introduction **ix**

I Scientific Paper **1**

List of Abbreviations

1D-BPP	One-Dimensional Bin Packing Problem
1D-BPP-W&B	One-Dimensional Bin Packing Problem and Weight and Balance
3D-BPP	Three-Dimensional Bin Packing Problem
%MAC	Percent Mean Aerodynamic Chord
AMS	Amsterdam Airport Schiphol
APP	Air Cargo Palletization Problem
BAX	Baggage
BF	Best-Fit
BPP	Bin Packing Problem
CG	Center of Gravity
COL	Cooling Storage
CRT	Controlled Room Temperature Storage
EP	Extreme Point
FF	First-Fit
FFD	First-Fit Decreasing
FRF	Fractional Relax-and-Fix
I&F	Insert-and-Fix
IAH	George Bush Intercontinental Airport
IATA	International Air Transport Association
ICN	Incheon International Airport
LAX	Los Angeles International Airport
LW	Landing Weight
MAC	Mean Aerodynamic Chord
MILP	Mixed Integer Linear Programming
MR	Max-Rest
NF	Next-Fit
NFD	Next-Fit Decreasing
NP	Non-Deterministic Polynomial-time
PAX	Passenger
R&F	Relax-and-Fix

RS	Residual Space
SIN	Singapore Changi Airport
TOW	Takeoff Weight
ULD	Unit Load Device
VLF	Volume Load Factor
W&B	Weight and Balance
WBP	Weight and Balance Problem
ZFW	Zero Fuel Weight

Introduction

The thesis, "Optimizing Fuel Efficiency in Intercontinental Passenger Flights: Integrating Air Cargo Palletization and Weight and Balance Problem," addresses the challenge of optimizing aircraft performance by strategically allocating cargo items to Unit Load Devices (ULDs) and their respective belly positions in intercontinental passenger flights. The primary goal is to enhance fuel efficiency by integrating the air cargo palletization problem with the weight and balance problem, aiming to maximize cargo load, improve the aircraft's center of gravity.

The project originated from the observation that current operational practices may only partially use the potential for optimizing aircraft performance through strategic cargo allocation. Developed in collaboration with Air France KLM Martinair Cargo, this research uses real-world data and operational contexts to address these challenges. The airline's involvement was crucial in understanding the practical constraints and opportunities within air cargo operations, driving the development of a robust optimization model.

What makes this project unique is its innovative approach to solving the palletization problem (assigning cargo to ULDs) and the weight and balance problem (positioning ULDs within the belly of the aircraft). The framework introduced employs a feedback loop between an integrated one-dimensional bin packing with weight and balance, solved with a mixed integer linear programming formulation, and a three-dimensional bin packing, solved with a heuristic. By integrating these two traditionally separate problems, the project enhances operational efficiency and contributes significantly to sustainability efforts. The project presents a method to increase fuel efficiency in the air cargo industry, supporting Air France KLM initiatives to reduce emissions.

This thesis report presents a scientific paper describing the integrated model's methodology, including the mathematical formulations and the results of testing and validating the model with actual data from Air France KLM Martinair Cargo.

I

Scientific Paper

Optimizing Fuel Efficiency in Intercontinental Passenger Flights: Integrating Air Cargo Palletization and Weight and Balance Problem

G.A.M. Puttaert*

Delft University of Technology, Delft, The Netherlands

Abstract

This paper presents a mathematical modeling framework designed for air cargo operations of a combination airline, focusing on intercontinental passenger aircraft. This framework optimizes the palletization problem (assigning cargo to Unit Load Devices (ULDs)) and the weight and balance problem (positioning ULDs within the belly of the aircraft). Unlike the traditional approach of solving these problems in sequence, our framework employs a feedback loop between an integrated one-dimensional bin packing with weight and balance and a three-dimensional bin packing. This feedback loop iteratively refines the solution by backpropagating information when items do not fit, reducing the solution space and computation time. The palletization problem is addressed with a three-dimensional bin packing heuristic, while the integrated one-dimensional bin packing and weight and balance problem is solved using a mixed integer linear programming formulation. The model employs a lexicographic optimization approach to prioritize maximizing the percent mean aerodynamic chord at zero fuel weight, leading to significant fuel reduction. Additionally, operational objectives aligned with our partner airline's practices are optimized to reflect actual operations. Scenario analyses validate the model, demonstrating potential fuel savings across various intercontinental routes and aircraft types, with an average fuel saving of 0.53% and reaching up to 1.90%, yielding substantial economic and environmental benefits.

1 Introduction

The air cargo industry is an essential part of international trade and logistics, facilitating the transportation of goods globally. A crucial element in the sector's operational efficiency is the use of Unit Load Devices (ULDs). These containers and pallets are designed to optimize the use of the cargo space in the bellies of freighter and passenger aircraft. Freighter aircraft are dedicated to transporting cargo, while passenger aircraft transport both cargo and passengers. In passenger aircraft, the baggage (BAX) ULDs for the passengers' BAX always have priority over the cargo ULDs. The strategic placement of the ULDs within the aircraft cargo hold is crucial to the aircraft's operational efficiency. The allocation of the BAX and cargo ULDs to a respective belly position in the aircraft cargo hold significantly affects the aircraft's Weight and Balance (W&B).

The W&B of an aircraft is a critical factor in its safety and performance, ensuring that the aircraft stays within the aircraft's type Center of Gravity (CG) and weight limits. The aircraft must remain within the limits to ensure that the aircraft can take off following the regulations, so a proper allocation of the ULDs is crucial. From a flight dynamics perspective, improper loading disturbs the aircraft's balance and aerodynamic efficiency. It affects the control surfaces' effectiveness and increases fuel consumption due to the need for additional lift and thrust, decreasing aircraft performance and efficiency. (Federal Aviation Administration, 2016)

This paper addresses the scope of passenger aircraft with intercontinental destinations for several reasons. Firstly, the impact of badly loaded aircraft in terms of W&B is more significant for long-haul flights, where fuel efficiency and balance are crucial for cost efficiency. Secondly, passenger aircraft constitute a considerable portion of flights for many airlines, making them a significant area for operational improvements. Thirdly, on domestic and continental flights, the cargo weight is small compared to the passenger (PAX) and BAX weight, making the impact of the cargo weight on the aircraft's W&B less significant. By focusing on intercontinental flights, the paper aims to address the challenges where they are most impactful by improving operational efficiency and sustainability of air cargo transport in the global airline industry.

Given these considerations, a challenge arises in assigning each ULD to the correct belly position in the passenger aircraft's belly to ensure optimal aircraft performance, known as the Weight and Balance Problem (WBP). In preparing an aircraft for an intercontinental flight, the WBP is not the only challenge. A series of

*MSc Student, Sustainable Air Transport, Faculty of Aerospace Engineering, Delft University of Technology

complex logistical challenges must be addressed before assigning the ULDs to their respective belly positions, beginning with the aircraft configuration problem, which determines the appropriate types and quantities of ULDs that will be loaded into the aircraft. Following this, the build-up scheduling problem requires precise planning to align when and where each ULD will be assembled. While these challenges are foundational, this paper will focus on the last logistical challenge before the ULDs can be loaded onto the aircraft: the Air Cargo Palletization Problem (APP), as identified by Brandt and Nickel (2019). This problem involves strategically selecting and packing cargo items into ULDs to optimize space while complying with constraints such as orientation, weight distribution, stacking, and grouping, all while respecting safety standards.

Recognizing the critical impact of the W&B on the aircraft's operational efficiency, this paper proposes an approach that integrates the APP with the WBP. In air cargo operations, building ULDs leads to and is distinct from the W&B calculations. This sequential approach often overlooks the potential fuel reduction that could be gained by considering these two problems together. By selecting specific cargo items for particular ULDs and placing them at their optimal belly position within the aircraft's cargo hold, it is possible to improve the aircraft's flight efficiency while maximizing cargo load.

This research utilizes a framework that adopts an approach with a feedback loop between an integrated one-dimensional bin packing problem (1D-BPP) and W&B alongside a three-dimensional bin packing problem (3D-BPP). The integrated 1D-BPP and W&B is modeled and solved with a Mixed Integer Linear Programming (MILP) formulation and serve as input in the second step, 3D-BPP, which is solved with a heuristic. The 3D-BPP heuristic is necessary to confirm that the items allocated in the integrated 1D-BPP and W&B fit the three-dimensional dimensions of the ULDs. If the 3D-BPP heuristic outputs deferred items, i.e., items that could not be packed in the ULD, the information is back-propagated through a feedback loop to solve the framework iteratively.

The rest of the paper is organized as follows. Section 2 introduces the relevant literature on the APP and the WBP. Section 3 presents the problem statement and methodology, detailing the 1D-BPP and W&B MILP model, the 3D-BPP heuristic, and the feedback loop. Section 4 describes the scenarios and instance types used for evaluating the model's performance. Section 5 discusses the scenario analysis results, and Section 6 concludes with the implications of the findings and suggestions for future research.

2 Literature Review

This section builds on the outlined problems and opportunities in the air cargo industry and reviews the literature on the APP and WBP. The literature review will address the WBP and its fundamental importance for the aircraft's operational efficiency. The APP will be discussed, focusing on the strategic selection and placement of cargo items in the ULDs.

2.1 Weight and Balance Problem

2.1.1 Preliminaries

The WBP is a critical aspect of the aviation industry in preparing every flight leg for each aircraft type around the globe. For the scope of this paper, the W&B of intercontinental passenger aircraft are controlled and monitored by an operational division of an airline, Load Control. A load controller is responsible for calculating the aircraft weight, balance, structural load limitation, and the aircraft's belly position configuration, assigning the set of ULDs. The job of the Load Control team is to ensure the safety and the aircraft's operational efficiency of every flight.

To further introduce the literature and, later, the methodology of this paper, two concepts and definitions must be introduced: The CG envelope and the Mean Aerodynamic Chord (MAC). The CG envelope of an aircraft type is defined as a non-linear function or envelope representing the aircraft's CG limits for a range of weights. An example of a CG envelope is shown in Figure 1(a).

The CG envelope evaluates three critical payload limits of the aircraft: Zero Fuel Weight (ZFW), Takeoff Weight (TOW), and Landing Weight (LW). ZFW represents the total weight of the aircraft and its contents, excluding fuel. TOW is the aircraft's weight at takeoff, incorporating all payloads and fuel, while LW is the aircraft's weight at landing after fuel consumption during the flight. The axes of the CG envelope are defined by weight and index. The index, displayed on the horizontal axis, is non-dimensional and expresses the moment caused by the aircraft's load. The weight is measured in kilograms. The load controller's primary responsibility is to ensure that the indexes for the three payloads remain within specified envelope limits. This ensures compliance with safety regulations and facilitates a safe takeoff.

Operational efficiency in aviation is linked to the CG envelope. The MAC is central to this relationship, a two-dimensional representation of the aircraft's wing as illustrated in Figure 1(b). The position of the CG relative to the MAC is expressed as a percentage of the distance from the MAC's leading edge to the CG, denoted as Percent Mean Aerodynamic Chord (%MAC).

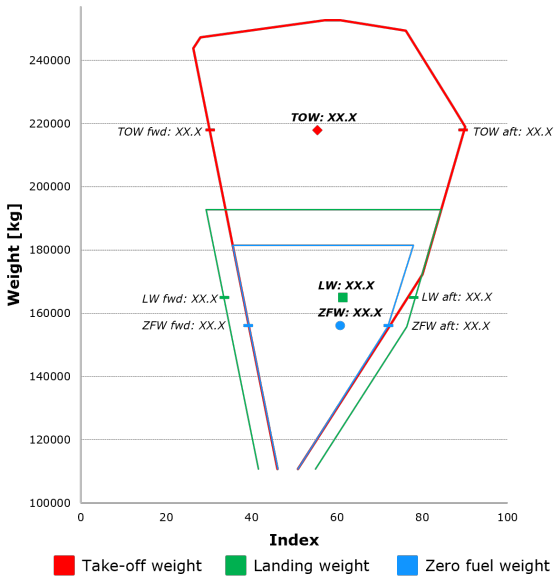

(a) Example of a CG Envelope (limits and indexes are not disclosed due to confidentiality)

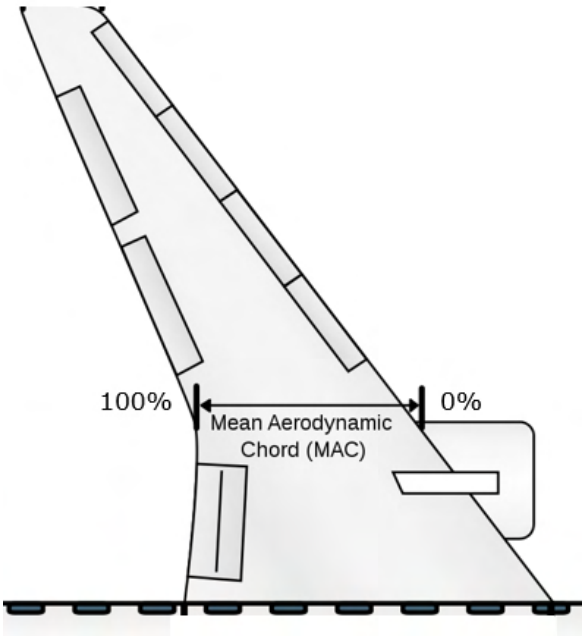

(b) Illustration of MAC

Figure 1: Important concepts for the WBP.

Among these, %MAC at ZFW is particularly crucial due to its significant impact on the aircraft's aerodynamic efficiency throughout the flight. Positioning the ZFW index as close as possible to the rear (aft) limit of the ZFW CG envelope results in a higher %MAC at ZFW and decreases the aircraft's drag, thereby enhancing operational efficiency through reduced fuel consumption. (Federal Aviation Administration, 2016). Unlike the %MAC at TOW and LW, which are influenced by fuel burn during the flight, %MAC at ZFW remains close to constant, providing a more stable reference for optimizing the aircraft's W&B. With this understanding, the WBP is defined as optimizing cargo load to maximize %MAC at ZFW while satisfying the CG envelope and the aircraft's structural and safety constraints.

2.1.2 Relevant Work

Building on the challenge of the WBP, Limbourg et al. (2012) paper was the first to present a MILP problem developed for optimal loading of ULDs into an aircraft. This approach was innovative in integrating the moment of inertia into the model, thereby optimizing the moment of inertia of the aircraft under the CG constraints. The model also incorporated various constraints critical for aircraft safety, such as lateral balance, feasibility envelopes based on the aircraft's structural capabilities, combined and cumulative load limits, and a specialized constraint for the Boeing 747's body cumulative load limit. Limbourg concluded from his case study with real-world data that the model's effectiveness is better than manual planning and costs significantly less time.

Vancroonenburg et al. (2014) highlighted the importance of considering various constraints to ensure the structural integrity, stability, safety of the cargo, and operational efficiency. Their model addresses various constraints, including the weight and dimensions of ULDs and the importance of the CG. Vancrooneneburg et al. were the first to design the WBP model with the primary goal of maximizing the cargo load and a secondary goal of minimizing the deviation from the aircraft's center of gravity expressed in %MAC. The model uniquely combines aspects of a knapsack problem, load balancing, and integrating several real-life features such as overlapping loading configurations, oversized containers, and cargo priority. Vancroonenburg et al.'s work significantly advances the WBP field.

Zhao et al. (2021) introduced an innovative approach to the WBP, highlighting aircraft safety, operational efficiency, and profit. Their work is different in considering the aircraft's CG envelope as a key constraint, a concept not explored in depth in prior research. The model maximizes the payload and optimizes the CG using a mixed integer programming method. The CG envelope constraints define the minimum and maximum CG limits for varying aircraft weights, addressing the risks associated with previous research that used a constant delta to limit the CG envelope. By adding the CG envelope constraints to the WBP, Zhao and colleagues made the WBP more realistic.

In a more recent study, Lu et al. (2023) addressed the WBP with a multi-objective mixed integer programming model focusing on maximizing cargo load and minimizing the CG deviation. A new aspect added to the literature from their approach is a genetic algorithm, which improves the optimization process by adopting strategies such as a fitness function. Their model was tested with a case study that looked at a B777 Freighter and concluded that it had a better loading solution than manual loading by the load controller. This paper advanced the literature on the WBP by studying and implementing optimization algorithms for this problem.

2.2 Air Cargo Palletization Problem

As identified by Brandt and Nickel (2019), the APP is crucial problem before the WBP. In the air cargo industry, every volume and cargo item counts, making efficient palletization necessary for profitability. Literature on the APP explores various strategies, algorithms, and models to optimize cargo load. The APP's main goal is to assign cargo items within ULDs to maximize load while ensuring constraints are satisfied. The most researched problem in this context is the bin packing problem (BPP), which has evolved from a 1D-BPP to a 3D-BPP. Each dimension adds complexity and realism, resembling real-life cargo packing in ULDs. This evolution demonstrates the industry's ongoing efforts to maximize cargo load.

The challenge of the BPP is to develop efficient and executable strategies and models to solve problems resembling real-life scenarios in a manageable computational time. Rieck presented heuristics algorithms to decrease the problem optimization time of the 1D-BPP. The BPP is a problem in which the computational time of the problem increases with its complexity or increases in problem size. This is why the development of heuristics algorithms is essential to solve such problems. The heuristics algorithms presented in the paper are based on First-Fit (Decreasing), Max-Rest, Next-Fit (Decreasing), and Best-Fit (Reick, 2021).

First-Fit (FF) and First-Fit Decreasing (FFD) Algorithm:
The FF algorithm processes all items i. If item i fits ULD j, it is packed in ULD j. If item i does not fit in any available ULD j, a new ULD j is created, and item i is packed. The FFD algorithm first sorts the items i in decreasing order regarding their weight and then applies the same step as the FF algorithm.

Max-Rest (MR) Algorithm:
The algorithm defines the ULD j with the most remaining capacity S. If the item i fits the ULD j, the item i is packed. If not, a new ULD j is created, and the item i is packed.

Next-Fit (NF) and Next-Fit Decreasing (NFD) Algorithm:
The NF algorithm places the items i in the order they arrive and places item i into the current ULD j if it fits. If it does not, the ULD j is closed, creating a new ULD j. The NFD algorithm first sorts the items i in decreasing order regarding their weight and then applies the same step as the NF algorithm.

Best-Fit (BF) Algorithm:
If item i fits ULD j, it is placed in ULD j, and the remaining capacity of ULD j is calculated. If item i does not fit, pack item i in the ULD j with the minimum remaining capacity after adding item i. If no such ULD exists, open a new ULD.

The BPP's complexity extends to how much the problem resembles the real-world scenario. Paquay et al. developed a mixed integer programming model to optimize the loading of cargo items into ULDs, focusing on the three-dimensional multiple bin size BPP.(Paquay et al., 2014) This model integrates constraints encountered in real-world applications, particularly in air transportation. The main objective of their model is to minimize the volume of utilized ULDs while satisfying a multitude of constraints, such as ensuring no overlap of items and the container weight limit. Of particular relevance to air cargo applications, the model also considers the unique shapes of ULDs, as some ULDs have specific shapes to fit the belly of aircraft. Additionally, the model integrates considerations for cargo stability, both static and dynamic, and load-bearing strength, which are crucial for ensuring the safety and integrity of the cargo during transportation. The study also emphasizes the importance of weight distribution within each ULD and across the aircraft to meet the technical and safety standards of the airline industry. Paquay's work represents a significant advancement in the field, offering a realistic representation of the 3D-BPP and providing a basis for developing new heuristics aimed at practical, real-world applications.

Building on earlier work, Paquay and Oliveria introduced in 2018 a mixed integer programming-based constructive heuristics aimed at improving the efficiency and practicality of the model (Paquay et al., 2018). To address the computational challenges posed by the model's numerous integer variables, Paquay developed three distinct heuristics: Relax-and-Fix (R&F), Insert-and-Fix (I&F), and Fractional Relax-and-Fix (FRF). These heuristics were designed to construct initial solutions more efficiently while keeping the original model's comprehensive nature. The R&F heuristic simplifies the problem by sequentially solving smaller MIPs, each time relaxing the integrality constraint on a subset of variables using a branch and bound method. The I&F heuristic

introduces an approach of iteratively inserting boxes into ULDs, maintaining the integrality of all variables throughout the process. The difference between the R&F and I&F methods is that the I&F does not consider all variables at every iteration, and the integrality constraints are never relaxed. The FRF heuristic merges the strategies of R&F and I&F, selectively relaxing the integrality constraints of certain variables iteratively. The introduction of these heuristics methods marks an advancement in the field, offering practical strategies. The paper concluded that these heuristic methods are promising because they quickly compute feasible solutions for the problem.

Despite advancements in addressing the WBP and the APP, the current literature often considers these problems distinct and separate. Specifically, an integrated approach is absent in the context of passenger aircraft, where the dual challenge of carrying passengers and cargo presents unique operational constraints. While considerable progress has been made in each problem individually, with sophisticated algorithms and complex models, an integrated framework that simultaneously addresses both the APP and WBP for passenger aircraft is still needed.

This research aims to fill this literature gap by proposing an integrated model that combines the APP with the WBP. By optimizing the placement of cargo items within ULDs and their corresponding positions in the belly of passenger aircraft, this study aims to enhance fuel efficiency. This approach with a feedback loop addresses a critical need in the air cargo industry and could improve fuel savings. The framework of the proposed model will be discussed in the next section.

3 Problem Statement and Methodology

This paper aims to optimize the %MAC at ZFW for intercontinental passenger aircraft by integrating the APP and WBP, considering the aircraft type, fuel, set of cargo items, set of BAX, and the seat map of the PAX while respecting operational objectives and safety constraints. The methodology used to solve this problem is composed of two main models. The first is an integrated 1D-BPP and W&B MILP model that serves as an input for the second model, a 3D-BPP heuristic. If the 3D-BPP outputs deferred items, i.e., items that could not be packed, the information from the second model is back-propagated into the first one via a feedback loop so that the two models iteratively optimize the process. A fully integrated approach combining a 3D-BPP and W&B into a MILP model was not chosen due to its significant computational time. By separating the problem into two models, the methodology allows for more efficient computation and quicker iterative optimization. The methodology flowchart to solve this problem can be seen in Figure 2.

The methodology to solve the problem begins with the input data blocks, consisting of fuel, aircraft, cargo, PAX, and BAX data. This data is used in the 1D-BPP and W&B (1D-BPP-W&B) block. This block is crucial as it sets the foundation of the problem by outputting the ULDs configuration and their placement in the belly and calculates the %MAC at ZFW for the specific flight. Following this, the 3D-BPP block takes the output from the 1D-BPP-W&B block to solve the 3D-BPP for these configurations, ensuring that the cargo items' three-dimensional dimensions fit within the ULDs. The feedback loop is activated if the 3D-BPP block outputs items that could not have been packed, called deferred items. This loop will be explained in detail later in the section. If no deferred items are found, a feasible solution is found. All items fit into the ULDs and can be loaded onto the aircraft, respecting the belly configuration to obtain the optimal %MAC at ZFW.

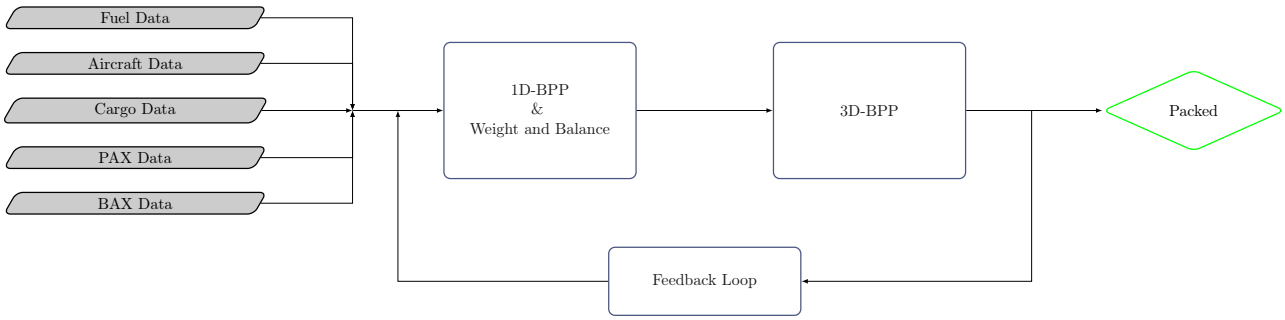

Figure 2: Methodology flowchart

3.1 Input Data

The problem-solving process relies on key data sets that address the APP and WBP. This subsection details the primary data types: cargo, PAX, BAX, fuel, and aircraft, and their roles in the methodology. Cargo data contains booking numbers, dimensions, weight, and specific handling requirements, influencing aircraft belly configurations. Handling constraints, such as stackability, rotatability, dangerous nature, and temperature

sensitivity, are considered in the 1D-BPP-W&B block. ULD information includes type and quantity per flight, with varying dimensions and weight limits. PAX data provides information about PAX count and seat map configurations. The seat map determines the distribution of passengers and their respective weights across different compartments. The International Air Transport Association (IATA) provides standardized weight values, setting each PAX at 84 kilograms. For intercontinental flights, BAX data includes the weight and type of BAX ULDs. Proper management ensures accurate loading and prioritization. Fuel data includes information about the fuel load. Aircraft data includes constants defining belly and overlapping positions, which differ according to aircraft type, ensuring ULDs are allocated accurately.

3.2 1D-BPP and Weight and Balance

The 1D-BPP-W&B block represents the initial step in the methodology flowchart. This block integrates the APP and the WBP into a unified approach solved with a MILP formulation, providing a comprehensive list of ULDs used and specifying which items are packed into each ULD. The resulting configuration then acts as input for the subsequent 3D-BPP block. This subsection details the mathematical model and explains how the constraints are formulated to address both problems simultaneously. The full mathematical formulation of the 1D-BPP-W&B is provided in Appendix A. The following focuses on the description of the main decision variables, objective functions, and constraint types.

Five decision variables are introduced to solve the 1D-BPP-W&B problem. The first decision variable p_{ij} is a binary variable that is unitary if item i is assigned to ULD j. The second decision variable u_j is a binary variable that is unitary if ULD j is used. The third decision variable f_{jt} is a binary variable that is unitary if ULD j is allocated to belly position t. Figure 3 illustrates an example of belly positions. The fourth decision variable SP_{b_i} is a binary variable that is unitary if any item i with the same booking number b_i is not assigned in the same ULD. The fifth decision variable w_{ijt} is a continuous variable that is the weight of item i assigned to ULD j at position t.

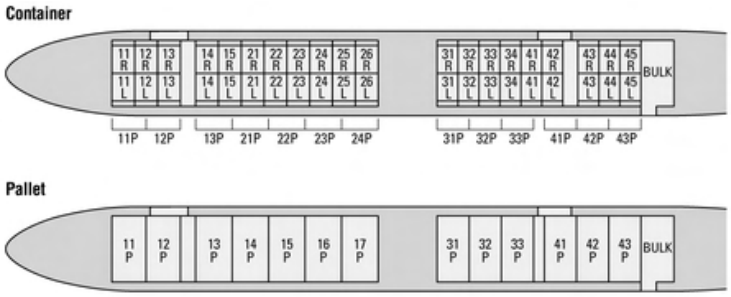

Figure 3: Belly positions of a Boeing 787-10 passenger aircraft. The upper section shows container positions, and the lower section shows pallet positions (All Nippon Airways Cargo, 2024).

With the decision variables specified, the next step is formulating the objective functions that optimize the 1D-BPP-W&B problem. A lexicographic optimization approach is employed, given the complexity and many aspects influencing the optimization process. In this approach, the objective functions are prioritized from highest to lowest, and each objective is optimized sequentially. The first objective is optimized, and its optimal value is added as a constraint in the subsequent optimizations, ensuring that each subsequent objective does not deteriorate the value of the higher-priority objectives.

The primary objective function is to maximize %MAC at ZFW. This objective function is essential for optimizing the aircraft's aerodynamic efficiency, reducing fuel consumption, and satisfying the CG envelopes of the different aircraft types. This involves strategically placing the decision variables w_{ijt} and the set of BAX, BUP, and T ULDs to their corresponding belly positions to yield the highest %MAC at ZFW while satisfying all constraints. BUP ULDs are ULDs built up and handed over ready for carriage by the shipper or the shipper's agent as complete units, while T ULDs are transfer ULDs that are not modified in the warehouse after being received by the sender. However, the complete formulation of this objective function specified in Equation 2 cannot be disclosed due to the confidentiality of our partner airline. The second objective is to place larger items in PMC/PAG ULDs and smaller items in AKE ULDs. This operational strategy ensures that ULD packing is realistic and reflects standard industry practices, as defined in Equation 3. The ULD types, PMC, PAG, and AKE, are specified in Appendix C. The third objective is to minimize the number of active ULDs. This objective function aims to reduce the number of ULDs used to pack all items i each with a volume v_i, ensuring efficient resource use, as defined in Equation 4. The fourth objective is to minimize the underutilization of ULDs. This objective function ensures that ULDs are opened when a minimum of 20% of the ULDs volume is used, if possible. This approach aligns with real-world practices and is defined in Equation 5. The fifth objective minimizes separating items with the same booking number across different ULDs through decision

variable SP_{b_i}, ensuring they are packed together to simulate operational practices, as defined in Equation 6. The final objective is to minimize the distance of BAX ULDs to the cargo doors of the aircraft. This objective function ensures they are placed near the cargo doors for efficient unloading at the arrival airport, aligning with real-world operational requirements, and is outlined in Equation 7.

Six objective functions have been introduced to ensure the model reflects the real-world operational objectives important to our partner airline. This approach aims to achieve ULD packing and belly configurations that closely mirror real-world operations and fully capture the potential improvements of this model compared to current operations. The objective functions and decision variables defined above are the foundation for solving the 1D-BPP-W&B problem. To make these objectives work, constraints must ensure that the solution complies with safety and operational requirements. The constraints are divided into four categories:

1D-BPP Constraints
The 1D-BPP constraints ensure that the cargo items are packed into the ULDs without exceeding the ULDs' weight and volume limits. These constraints also ensure that every item of the cargo item set is assigned. Constraint 8 ensures that the total weight of items assigned to a ULD does not exceed its weight capacity, while Constraint 9 ensures that the total volume of items assigned to a ULD does not exceed its volume capacity. Constraint 10 ensures that all cargo items are assigned to one ULD, and Constraint 11 ensures that cargo items are not assigned to BAX, BUP, or T ULDs.

W&B Constraints
The W&B constraints, specific to each aircraft type, are the most comprehensive set within the model, ensuring aircraft safety and operational compliance. The constraints address crucial aspects essential to the model and the aircraft's safety requirements, and they are divided into three subcategories: position constraints, weight constraints, and CG envelope constraints.

The position constraints, in addition to ensuring that each belly position accommodates only one ULD and that ULDs are allocated according to their type, also significantly prevent ULDs from being placed in overlapping positions that are already occupied. Constraint 12 ensures that each active ULD is loaded to one position, and Constraint 13 ensures that each position can hold only one ULD. Constraint 14 specifies that a ULD is selected and assigned to a position according to its type; if a ULD and a position do not match, the ULD cannot be assigned to that position. Constraint 15 ensures that every BAX, BUP, or T ULD must be loaded to exactly one position. Additionally, Constraint 16 addresses the issue of overlapping positions, ensuring that once one of these overlapping positions is occupied, the others can no longer be allocated.

The weight constraints are crucial for maintaining the structural integrity and balance of the aircraft. Constraint 21 ensures that the weight of a ULD assigned to a position does not exceed the maximum allowable weight for that position. Constraint 22 ensures that the weight in a compartment does not exceed the maximum allowable weight for that compartment. Similarly, Constraint 23 and 24 ensure that the weight in the forward and aft belly compartments, respectively, does not exceed the maximum allowable weight for those compartments.

Constraints 25 and 26 are lateral balance constraints, which maintain the aircraft's lateral balance by limiting the difference in weight between ULDs on the left and right sides to a specific constant for each aircraft type. The linearized form of the lateral balance constraints are outlined in Appendix A.2. The CG envelope constraints ensure that the weight distribution for ZFW, TOW, and LW remain within their respective safety envelopes. Constraint 27 defines the forward index limit for the CG envelope, ensuring the weight distribution does not cause the CG to move forward beyond safe limits. Constraint 28 defines the aft index limit for the CG envelope, ensuring the weight distribution does not cause the CG to move aft beyond safe limits. This compliance guarantees that the aircraft can safely take off, operate, and land, satisfying safety requirements.

Special Handling Constraints
The special handling constraints address the specific requirements for certain cargo items and ensure their proper placement within the aircraft. These constraints are critical for managing items that require controlled environments, such as cooling or room temperature storage, and ensuring specific aircraft configuration rules.

Constraint 29, valid for all aircraft types, ensures that items requiring cooling storage (COL) and items requiring controlled room temperature storage (CRT) are not placed within the same ULD. This constraint is crucial for maintaining the required environmental conditions for these sensitive items. Constraints 30 through 43 define the special handling constraints for the Boeing 777-200ER and 777-300ER. These constraints ensure that COL and CRT items are not placed together in the front or aft cargo holds, thereby preventing conflict in their storage requirements. Constraints 44 through 47 define the special handling constraints for the Boeing 787-9 and 787-10. These constraints ensure that COL and CRT items are not placed in the rear cargo hold, maintaining the aircraft type configuration rules.

These special handling constraints are essential for maintaining the integrity and safety of cargo items that require specific environmental conditions, ensuring they are correctly assigned according to the requirements of each aircraft type.

Linking Constraints
The linking constraints form the core of the 1D-BPP-W&B block, ensuring the integration of the two problems. The primary role of the linking constraints is to manage the allocation of cargo items to respective ULDs and belly positions through the decision variable w_{ijt}.

Constraint 17 ensures that w_{ijt} equals zero if item i is not assigned to ULD j through decision variable p_{ij}. This prevents any weight assignment to ULDs that are not assigned to carry that item. Constraint 18 ensures that w_{ijt} equals zero if ULD j is not assigned to position t through decision variable f_{jt}. This constraint prevents any weight assigned to a position without an assigned ULD. The third linking constraint, Constraint 19 ensures that w_{ijt} equals the actual weight of the item m_i only when both pij and f_{jt} are equal to one, confirming that the whole item weight is assigned to the ULD and belly position. This constraint is linearized in the model, with detailed linearization steps outlined in Appendix A.2. Finally, Constraint 20 ensures that w_{ijt} does not exceed the actual weight of item i, thus maintaining the integrity of the weight assignment.

These linking constraints allow the 1D-BPP-W&B problem to be integrated and solved simultaneously. They ensure that the cargo items are correctly packed into the ULDs and assigned to the belly positions in the aircraft. Together, the objective functions and constraints in this subsection establish the foundation of the 1D-BPP-W&B block, providing a comprehensive approach to solving the integrated APP and WBP.

3.3 3D-BPP

The 3D-BPP block, the second step in the methodology flowchart, uses the output of the 1D-BPP-W&B block to solve the 3D-BPP and verify that cargo items fit into the ULDs, ensuring the feasibility of the ULD configuration. Packing problems that consider more than one dimension are considered NP-hard. An NP-hard problem is a combinatorial optimization problem that is Non-Deterministic Polynomial-time (NP) Hard, meaning the problem is at least as challenging as the hardest known problems, and there is not an efficient solution available. Thus, solving the problem requires significant computational time. A traditional 3D-BPP constructed by a MILP model is not feasible to solve within a reasonable time frame. To address this issue, the 3D-BPP block uses a heuristic algorithm to solve the packing problem of the 1D-BPP-W&B block solution. The 1D-BPP-W&B block provides the ULD configuration and its cargo items as input to the 3D-BPP block, which then uses the heuristic algorithm to pack the cargo items into the ULDs in three dimensions. This block aims to ensure that the cargo items fit into the ULDs and that the ULD configuration is feasible. This check must be performed quickly to verify the belly configuration before loading the aircraft. The 3D-BPP block uses an algorithm called the Extreme Points (EP) heuristic to achieve this.

The main principle behind the EP heuristic is that for each ULD, a global list of EPs is constantly updated after the placement of each item. The EPs are used to find potential placement positions for the following items in the ULD. Defining some characteristics of cargo items is essential before diving into the EP heuristic logic. The cargo item characteristics that influence the packing solution of the 3D-BPP include non-stackable items, which cannot have other items placed on top of them and are placed last in the list to increase the chances of finding a feasible packing solution, and rotatable items, which can be placed in different orientations. All possible orientations in which a cargo item can be positioned in a ULD are shown in Figure 4.

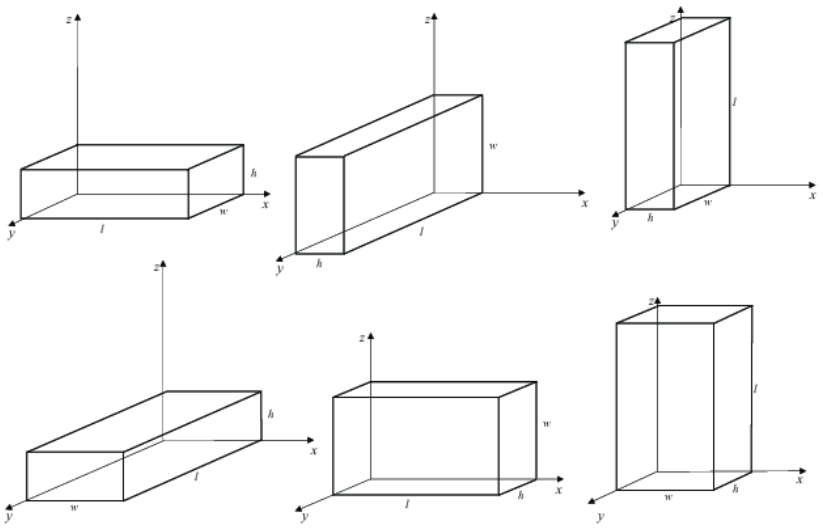

Figure 4: Cargo items' possible orientations in a ULD (Jozefowska et al., 2018)

The next step is understanding how the EPs are iteratively updated after each item is placed. The first EP created when a ULD is open is at coordinate $(0, 0, 0)$ for PMC and PAG ULDs and at coordinate $(a, 0, 0)$ for ULDs with a cut, such as AKE ULDs. In this context, a represents the length along the x-axis from the origin to the point where the cut begins, illustrated in Figure 5(b). Once the first item's back-bottom-left vertex is placed in the ULD at EP $(0, 0, 0)$ or $(a, 0, 0)$, the EP list updates to include potential positions for future items to be placed against or on top of the item. An example of EP generation is shown in Figure 5(a) and defined in Algorithm 2.

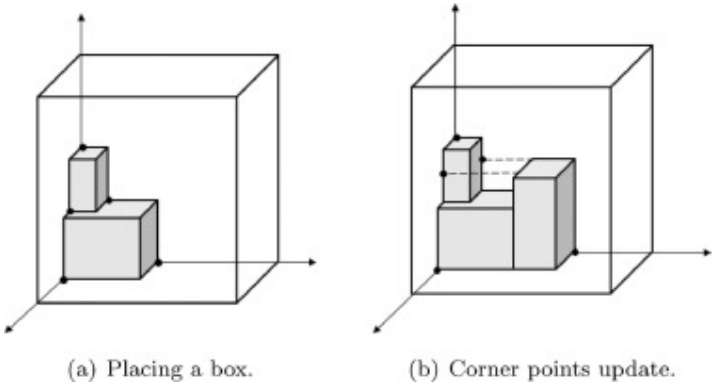

(a) Generation of the Extreme Points (Silva et al., 2019)

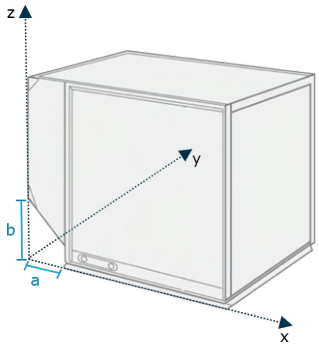

(b) Cut of AKE ULD

Figure 5: EP generation process

With an understanding of the cargo items' characteristics, the initial EP generation, and how the global EP list is updated, the following step is to understand how the EP heuristic decides which item to place first and in what order subsequent items should be placed in the ULD. The heuristic uses a merit function to accomplish this, aiming to maximize the utilization of the EP Residual Space (RS). The RS is the free space around the EP and consists of five components: RS_{left}, RS_{right}, RS_{front}, RS_{back}, and RS_{top}. Each component is measured as the distance between the EP and the ULD wall. The merit function is the sum of these components, as shown in Equation 1:

$$\text{Merit Function} = [(\text{RS}_{\text{left}} - l_{\text{item}}) + (\text{RS}_{\text{right}} - l_{\text{item}}) + (\text{RS}_{\text{front}} - w_{\text{item}}) + (\text{RS}_{\text{back}} - w_{\text{item}}) + (\text{RS}_{\text{top}} - h_{\text{item}})] \quad (1)$$

The merit function is calculated for each cargo item at each EP for all orientations of the cargo item. The algorithm prioritizes placing items on ground-level EPs (at the base of the ULD). If an item cannot be placed on a ground EP, it is attempted on non-ground EPs (on top of other items). This approach encourages the algorithm to prioritize ground placement. Each potential placement is checked against constraints like stability, fitting in the ULD, and collision with other items. The cargo item and orientation with the smallest non-negative merit function that satisfies all constraints is selected for placement. The process is repeated until all items are placed in the ULD and presented in detail in Algorithm 1. The framework for the algorithm presented for the 3D-BPP block is detailed in Algorithm 3.

3.4 Feedback Loop

The feedback loop is a critical intermediary between the 1D-BPP-W&B block and the 3D-BPP block. It is activated when the 3D-BPP block identifies deferred items, i.e., items that could have been packed but were not due to spatial or stability constraints. This loop is essential for iteratively adjusting the fit of all items into the ULD set and the ULD configuration output by the 1D-BPP-W&B block to optimize the %MAC at ZFW while satisfying all constraints. The flowchart detailing this process is illustrated in Figure 6 and will be discussed further in this section.

If deferred items are detected after the initial iteration, the ULDs, and their deferred items are re-evaluated through the ULD Block, as shown in Figure 7. This block is pivotal as it determines whether certain ULDs from the 1D-BPP-W&B configuration can be blocked in subsequent iterations, effectively reducing the solution space and computational time required to find a solution. Decisions within the ULD Block are grounded in operational practices and aim to reflect real-world scenarios.

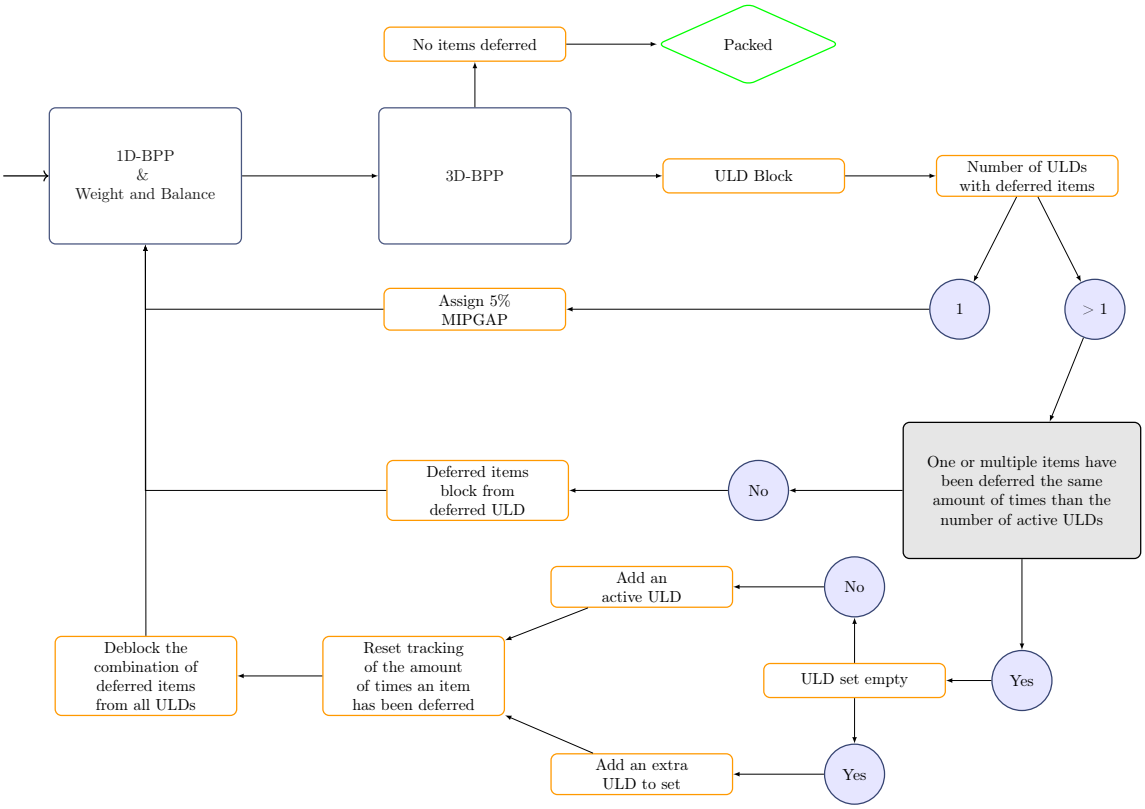

Figure 6: Feedback Loop flowchart

A key metric in this process is the Volume Load Factor (VLF), defined as the ratio of the total volume of items to the total volume of the ULD. The first decision point in the ULD Block assesses whether more than two ULDs remain not used, ensuring sufficient solution space is available to place deferred items in future iterations. If two or fewer ULDs are not used, the block exits, and the feedback loop proceeds.

If more than two ULDs are not used, the configuration of ULDs and their items is analyzed to identify any ULDs without deferred items and with a VLF of at least 65%. If this criterion is met for ULDs, they are blocked for the subsequent iterations. Conversely, if no ULDs meet this condition, those not blocked are individually evaluated to determine if they contain equal or fewer than two deferred items and have a VLF of at least 75%. ULDs meeting these criteria are then blocked for subsequent iterations, while those that do not meet the criteria continue through the feedback loop unblocked.

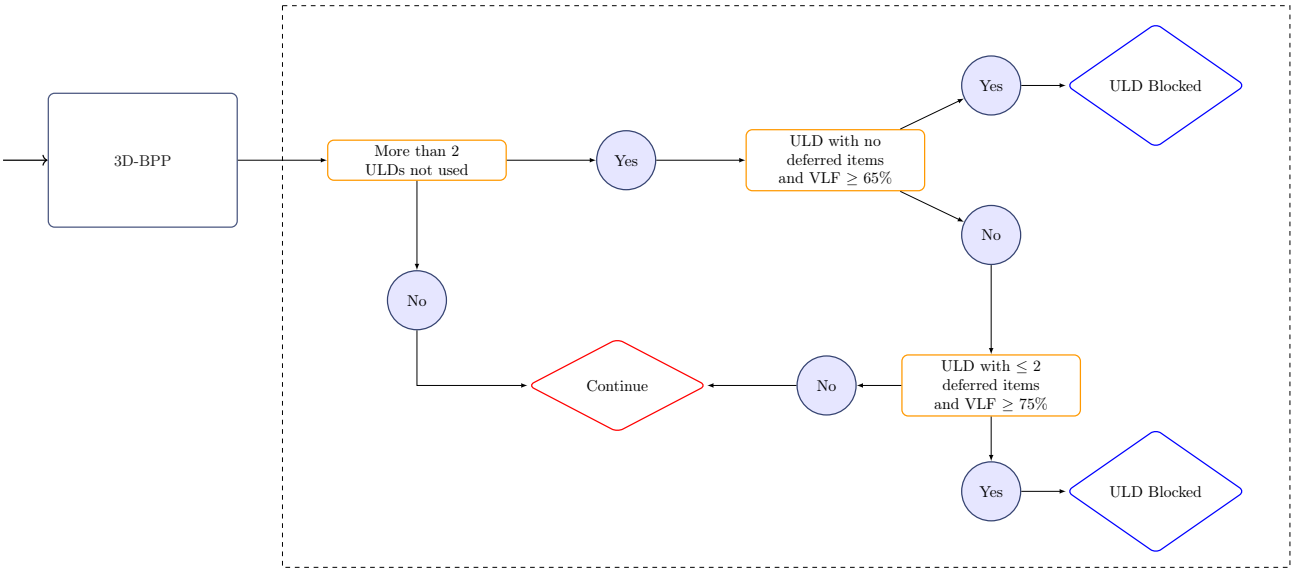

Figure 7: ULD Block flowchart

After assessing the ULD Block, the feedback loop progresses to the next stage in the feedback loop flowchart, focusing on evaluating the number of ULDs containing deferred items. If more than one ULD has deferred items, the feedback loop advances to the next step. However, if only one ULD contains deferred items, the feedback loop introduces a 5% MIPGap to the 1D-BPP-W&B block. This adjustment slightly relaxes the solution space, acknowledging that the solution is approaching a feasible configuration previously inputted into the feedback loop. The feedback loop then advances to a critical decision point. Given that an essential objective function of the model is to minimize the number of active ULDs, it is crucial to determine whether to open new or additional ULDs from the initial set allocated to the flight. This decision involves assessing whether one or multiple items have been deferred as often as the number of active ULDs. If an item has been deferred from all active ULDs, it will unlikely be packed within them. If this condition is not met, the feedback loop opts not to open new ULDs but instead blocks the combination of items that failed to be packed in all ULDs of the same type. This approach prevents overly constraining the solution space, allowing the model to find a feasible solution within reasonable computational time without repeating failed combinations.

If the condition is met, the feedback loop checks if the initial set of ULDs allocated to the flight is empty. If the set is empty, the loop adds an extra PMC and AKE ULD to the set. This ensures the solution space remains flexible, allowing allocation to achieve the optimal %MAC at ZFW. If the ULD set is not empty, the loop activates an additional ULD within the set, expanding the solution space and enhancing the chance of finding a feasible solution. Upon opening a new or additional ULD, the feedback loop resets the count of deferred items and lifts the block on deferred item combinations, allowing the model to re-optimize with the newly added ULD or ULDs.

The feedback loop ties the 1D-BPP-W&B block and the 3D-BPP block, ensuring that the solution space is not overly constrained and that the model can find a feasible solution within a reasonable computational time. The feedback loop's decisions are grounded in operational practices and real-world scenarios, ensuring the model's output is feasible and reflects industry standards.

4 Description of Scenarios and Instance Types

After outlining the model's methodology and components that address the integrated APP and WBP, the subsequent phase involves evaluating the model's performance through a detailed scenario analysis. This analysis assesses the model's effectiveness in optimizing %MAC at ZFW by strategically allocating cargo items into ULDs and belly positions. The scenario analysis compares the model's outputs across three scenarios: sequential, W&B-focused, and actual scenarios, and will be explored in detail in this section.

The critical scenario is the sequential scenario, which analyzes the model's performance. This scenario represents the sequence of the conventional operations where ULDs are first built, addressing the APP utilizing the 1D-BPP and 3D-BPP methodology and later optimized within the W&B context. This scenario uses the same objective functions and constraints as the integrated model but differs in the optimization sequence. The sequential scenario is introduced in this analysis to compare and analyze the impact of the strategic assignment of items in the ULDs and belly positions on the %MAC at ZFW as achieved by the integrated model.

The W&B-focused scenario is the second scenario in the analysis. This scenario evaluates the performance of the loading and belly configuration of real-world operations by reconfiguring the belly configuration of the actual flight using the actual ULDs that were built for the flight. This scenario assesses the potential improvements in W&B if the actual belly configuration of the flight had been optimized, highlighting the gap between current operations and the improvements that can be achieved by only optimizing the W&B without changing the ULDs themselves.

The actual scenario, the final scenario in the scenario analysis, represents the real-world conditions of the aircraft at takeoff, as provided by our partner airline. It provides a standard for understanding how the aircraft was loaded and its configuration's effectiveness under standard operational conditions.

After defining the scenarios, the following step involves selecting the destinations for which the model will be applied. This selection is crucial to test the model's performance across different aircraft types and continents, ensuring diverse cargo items' dimensions and weights. Additionally, it assesses the model's robustness in optimizing for various possible belly configurations along with weight limits and particular handling constraints per aircraft type.

The flights chosen for the scenario analysis originate from our partner airline's hub, Amsterdam Airport Schiphol (AMS). The selected destinations include Los Angeles International Airport (LAX), Singapore Changi Airport (SIN), George Bush Intercontinental Airport (IAH), and Incheon International Airport (ICN), each providing a unique set of challenges. These destinations are illustrated on the map in Figure 8.

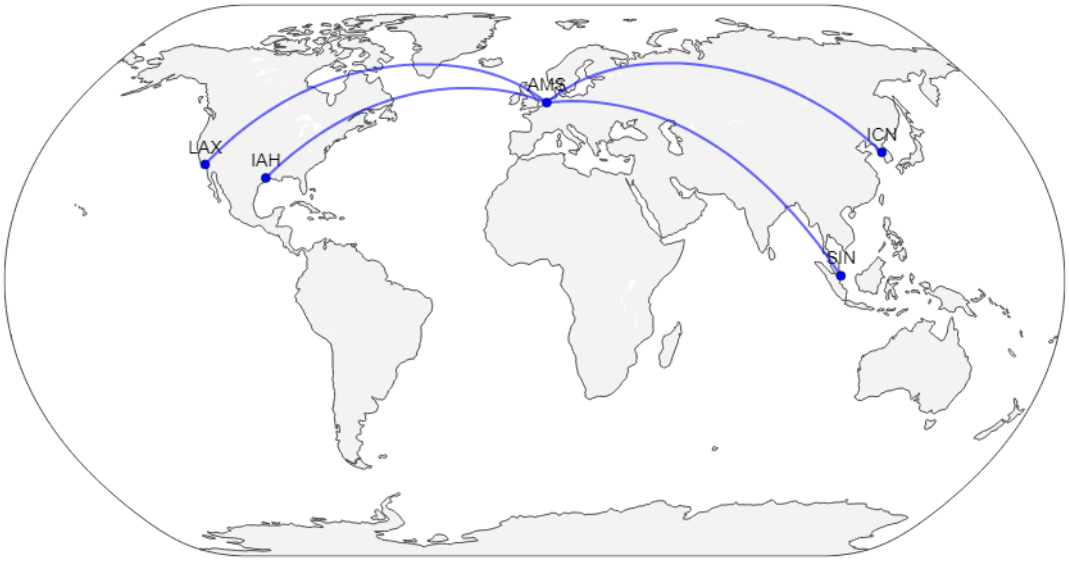

Figure 8: Selected destinations for the scenario analysis

The selected destinations introduce various aircraft types, including the Boeing 777-300ER, Boeing 787-9, Boeing 777-200ER, and Boeing 787-10. These aircraft and destinations are chosen to test the model's robustness across different types and their respective belly configurations, W&B constraints, and the different amounts and characteristics of cargo items. After selecting the destinations based on aircraft types and cargo item variations, the timeframe for the flights is established. The first quarter of 2024 is chosen to provide a sufficiently large sample size, containing 138 flights, enabling a comprehensive evaluation of the model's performance across various aircraft types, destinations, and many operational scenarios. The distribution of the destinations and aircraft types across the 138 flights are presented in Figure 9

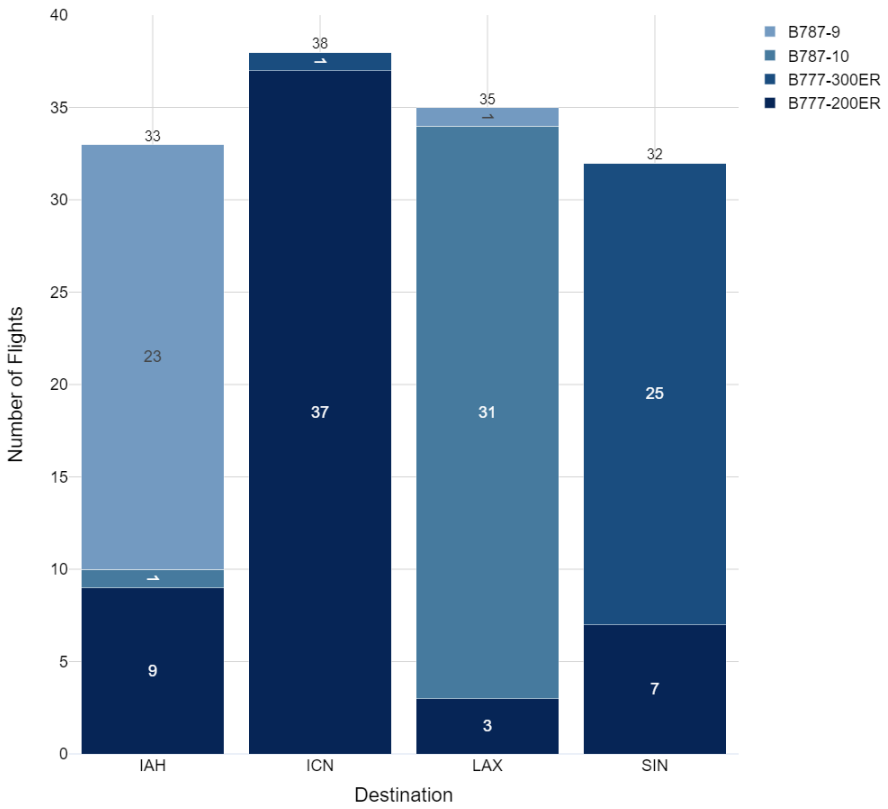

Figure 9: Distribution of aircraft types per destination in the set of flights

In addition to the distribution of aircraft types per destination, understanding the distribution of the number of cargo items for each aircraft type is essential. The histograms in Figure 10 illustrate the frequency distribution of the number of cargo items for each aircraft type used in the scenario analysis. On average, 110 cargo items were transported on the flights considered in this work, with a maximum of 380 items. These frequency distributions ensure a comprehensive evaluation of the different scenario performances.

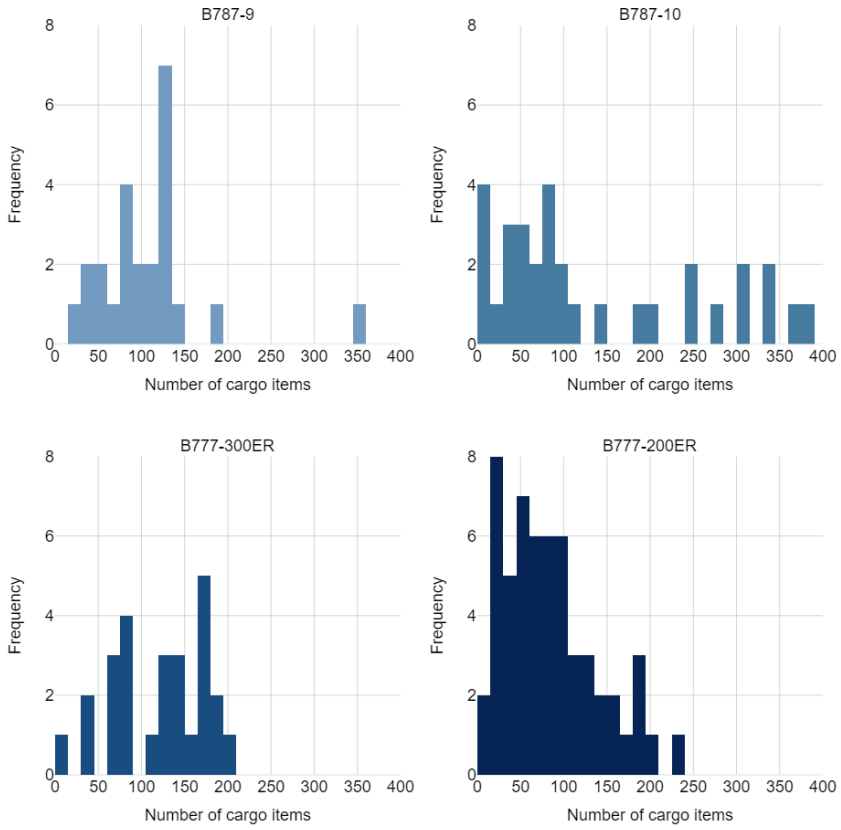

Figure 10: Frequency distribution of the number of cargo items for each aircraft type

Following the definition of scenarios, destinations, aircraft types, and timeframe, the next phase involves running the model for each specific scenario and destination. The outcomes are presented and analyzed in the subsequent section to assess the model's effectiveness across diverse flights and against the sequential, W&B-focused, and actual scenarios.

5 Results

This section presents the findings of the detailed scenario analysis, which evaluated the model's performance across the selected destinations. Each scenario is examined in terms of its impact on fuel efficiency, %MAC at ZFW. To understand the scenario analysis results, it is crucial to comprehend the model's output for each flight first. This understanding will provide a solid foundation for interpreting the scenarios results for the 138 flights.

Software and Hardware Specifications
All algorithms referred to in this paper are coded in Python 3.11.9, using libraries such as NumPy, pandas for data processing, and the Gurobi Optimizer 11.0 for solving the MILP model of the integrated 1D-BPP and W&B. Visualizations were created using Matplotlib and Plotly, with development carried out in Jupyter Notebooks. Data management was facilitated with an SQL database. The hardware configuration included a Lenovo ThinkPad T16 Gen 1 with a 12th Gen Intel Core i7-1265U processor (1.80GHz, 10 cores), 32 GB of installed physical memory, running on Microsoft Windows 10 Enterprise. This setup ensured efficient handling of the computational tasks and resulted in an average computational time of 7.5 minutes for the model. In comparison, the sequential scenario averages 3 minutes, and the W&B-focused scenario completes in 0.5 minutes. Furthermore, the model demonstrated its ability to handle the largest cargo items set, composed of 380 items, in 13 minutes, showing its ability to handle larger sets efficiently.

The model output for each flight includes visualizations of the 3D-BPP for the constructed ULDs and the CG envelopes, showcasing the envelopes for the optimal aircraft W&B. The 3D-BPP visualization offers a detailed view of how cargo items are packed within the ULDs, confirming their fit and packing in terms of special handling constraints. An example of the 3D-BPP output is shown in Figure 11.

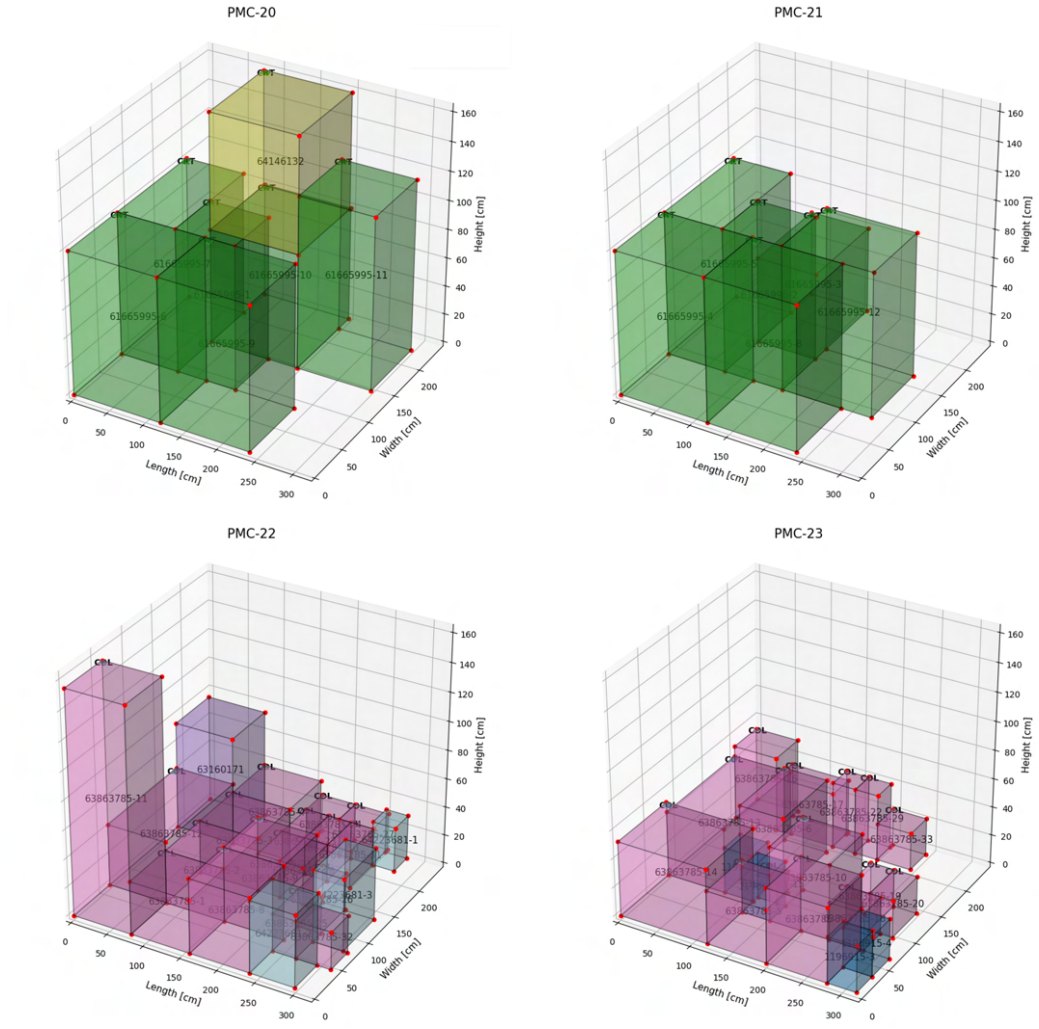

Figure 11: Visualization of the 3D-BPP results for the built ULDs of one of the flights tested in this work

The key results from an individual flight analysis focus on the %MAC at ZFW, detailing the arrangement of ULDs within the belly of the aircraft and the corresponding CG envelopes. For each flight, the optimal %MAC at ZFW is compared with the actual %MAC at ZFW to assess the model's efficacy and the impact of strategic cargo placement within the ULDs and belly positions on the aircraft's fuel efficiency. The CG envelopes' visualizations illustrate the aircraft's W&B, ensuring compliance with the aircraft's CG limits. The CG envelopes include three envelopes corresponding to the three payloads: TOW, represented by the red envelope, LW, represented by the green envelope, and ZFW, represented by the blue envelope. For safety constraints, the index of each payload must stay inside its respective envelope. An example visualization of the CG envelopes is presented in Figure 12.

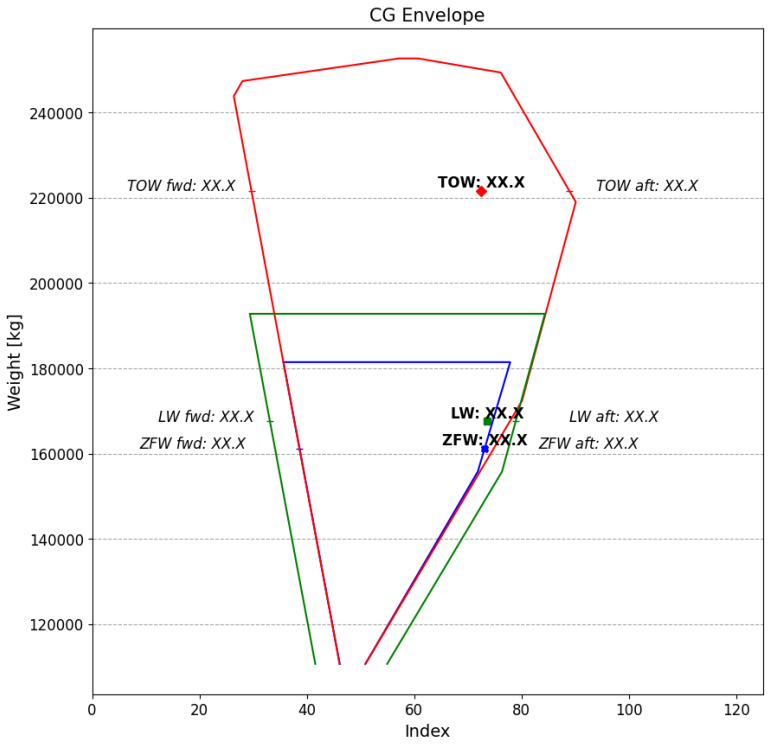

Figure 12: Visualization of the CG envelopes for one of the flights considered in this work (limits and indexes are not disclosed due to confidentiality)

The scenario analysis results are presented upon establishing a clear understanding of the model outputs for an individual flight. This analysis evaluates the performance across the model, sequential, W&B-focused, and actual scenarios for each selected destination and aircraft type. Initially, the results for the %MAC at ZFW for the 138 analyzed flights are reviewed. These findings are detailed in Figure 13, which showcases the %MAC at ZFW for the various destinations and aircraft types.

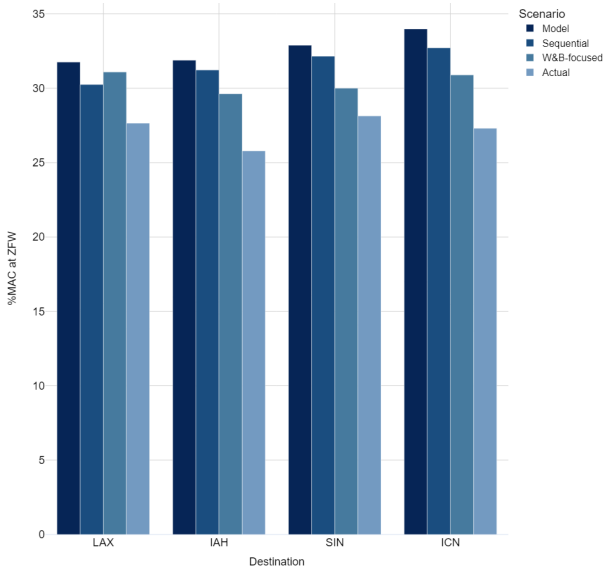

(a) %MAC for the scenario analysis for each destination

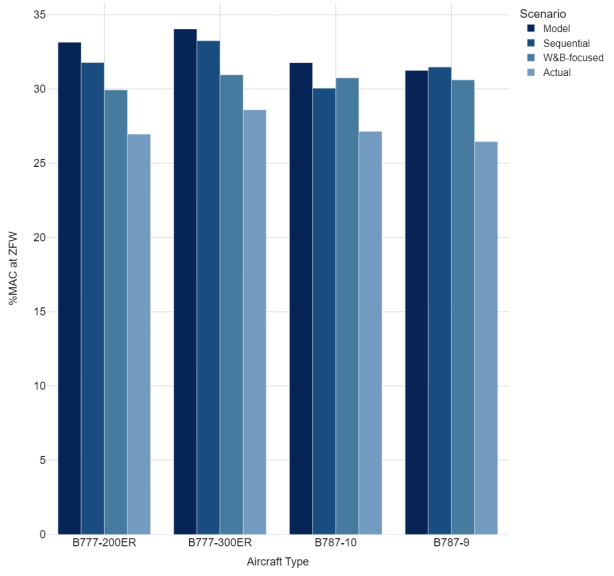

(b) %MAC for the scenario analysis for each aircraft type

Figure 13: %MAC at ZFW results of the scenario analysis for destinations and aircraft types

The results presented in Figure 13 demonstrate the model's robust capability to optimize %MAC at ZFW across diverse destinations and aircraft types. This analysis underscores the model's effectiveness in strategically allocating cargo items within ULDs and belly positions, enhancing the %MAC at ZFW for the model. A consistent enhancement in performance is observed, indicating that the model achieves further optimization

with increased complexity. The W&B-focused scenario shows an improved %MAC at ZFW by strategically reallocating the ULDs used in the actual scenario, thus achieving a better aircraft W&B.

Notably, complex and larger aircraft types such as the Boeing 777-300ER and Boeing 777-200ER demonstrate superior optimization of the %MAC at ZFW through the model compared to the actual %MAC at ZFW. This superior performance is linked to these aircraft's more intricate belly position configurations and larger maximum weight allocation, resulting in a broader ZFW CG envelope. This configuration provides a larger optimization space for the model, resulting in a more apparent difference between the modeled and actual %MAC at ZFW. For the larger aircraft types, such as the Boeing 777-300ER and Boeing 777-200ER, the model enhances the %MAC at ZFW on average by 5.44 and 6.18 percentage points, respectively, compared to an average increase of 4.63 and 4.79 percentage points for the aircraft types with narrower CG envelopes, the Boeing 787-10 and 787-9.

However, the sequential scenario performs better than the model for the Boeing 787-9. This is due to the sequential scenario employing fewer ULDs than the model, which reduces the number of ULDs to be assigned a belly position and expands the available solution space for strategically positioning ULDs towards the aircraft's rear compartments. Additionally, the CG envelope of the Boeing 787-9 is the narrowest of all aircraft types, limiting the model's ability to optimize the %MAC at ZFW compared to the other aircraft types. This resulted in a 0.23 percentage point enhancement on average for the Boeing 787-9 sequential scenario compared to the model.

The next phase of the scenario analysis examines the reasons behind the model's superior performance over other scenarios. Figure 14 provides a detailed analysis of the percentage weight distribution across the aircraft's compartments, highlighting how cargo ULDs and BAX are allocated within the belly compartments across the scenarios. An example of the belly compartments of an aircraft is illustrated in Figure 15, which provides context for the weight distribution analysis.

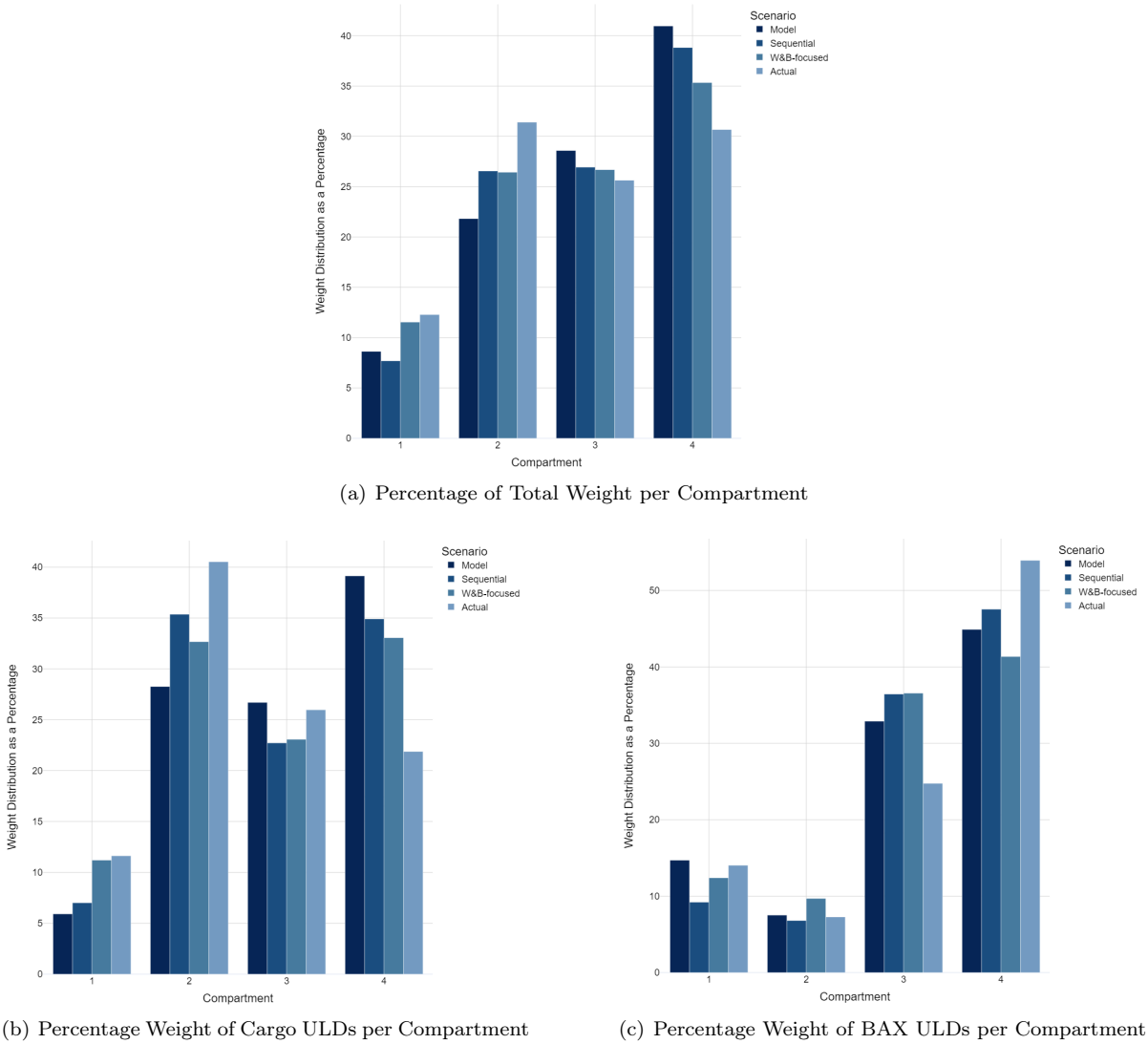

(a) Percentage of Total Weight per Compartment

(b) Percentage Weight of Cargo ULDs per Compartment

(c) Percentage Weight of BAX ULDs per Compartment

Figure 14: Weight distribution as a percentage across the aircraft compartments

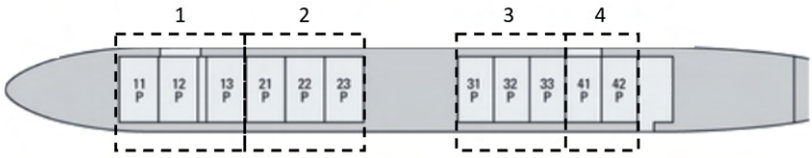

Figure 15: Belly compartments of an aircraft

The analysis reveals a strategic preference within the model to assign the most weight in compartment 4, effectively shifting the W&B towards the aircraft's aft limit of the ZFW CG envelope. In comparison, the actual scenario typically assigns cargo ULDs to compartment 2.

Conversely, BAX ULDs are placed in compartment 4 in actual operations, as opposed to compartment 2 in the model. This difference between the model's strategy and actual practice highlights significant opportunities for operational improvements. By reallocating BAX to compartment 2 and cargo ULDs to compartment 4, as the model suggests, the aircraft's W&B can be further optimized. This adjustment can enhance fuel efficiency by maintaining a more ideal distribution of weight across the aircraft's belly compartments.

The final phase of the scenario analysis focuses on the fuel deviations per scenario compared to the actual scenario, alongside the potential fuel savings achievable through each scenario's optimization. The fuel deviation analysis is presented in Figure 16, which features a boxplot chart illustrating the fuel deviation for the model, sequential, and W&B-focused scenarios. The analysis highlights that the model consistently outperforms the sequential and W&B-focused scenarios, achieving significantly higher fuel savings across the 138 flights. This enhanced performance is mainly due to the model's strategic placement of cargo items within their corresponding ULDs and positioning in the aircraft's belly, significantly enhancing the aircraft's W&B and %MAC at ZFW.

Optimization of the aircraft's W&B by the model leads to better fuel efficiency when compared to the sequential and W&B-focused scenarios. On average, the model achieves a fuel saving of 352 kg per flight, outperforming the sequential scenario's 268 kg and the W&B-focused scenario's 177 kg. Given that our partner airline operates around 1,500 flights per year towards the selected destination, this could save the airline an estimated 528,000 kg of fuel per year with the integrated model.

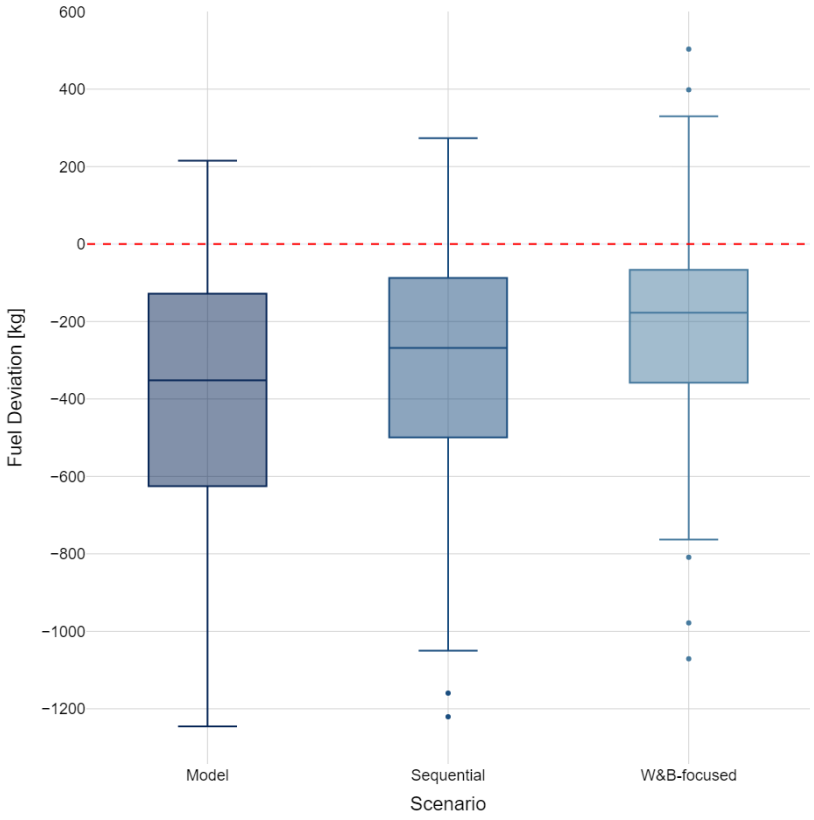

Figure 16: Fuel deviation analysis for the scenario analysis

The detailed scenario analysis has effectively demonstrated the model's ability to optimize the integrated APP and WBP. Across 138 flights, the model outperforms the sequential and W&B-focused scenarios, with average fuel savings compared to the actual scenario of 0.53% for the model compared to 0.41% for the sequential and 0.32% for the W&B-focused scenario. Notably, the most significant fuel savings observed with the model reached up to 1245 kg for larger and more complex aircraft types like the Boeing 777-300ER.

The findings from the scenario analysis demonstrate the benefits of an integrated APP and WBP model. Strategic allocation of cargo items to their corresponding ULDs and belly positions enhances the aircraft's W&B, improving fuel efficiency. The subsequent phase will explore the implications of these results and discuss the potential benefits for the airline industry in the conclusion section.

6 Conclusions

This paper presents a comprehensive approach to improving the fuel efficiency of intercontinental passenger aircraft by integrating the APP and the WBP. The model's robustness in optimizing fuel efficiency was validated through scenario analysis across various aircraft types and destinations, addressing challenges like diverse cargo item dimensions, weight, special handling constraints, and aircraft types' belly configurations.

The results highlight the model's capability to optimize %MAC at ZFW. The model demonstrated an average fuel saving of 0.53% per flight, with the most significant savings observed at 1245 kg for larger aircraft such as the Boeing 777-300ER. This underscores the strategic value of integrating the APP and the WBP by allocating cargo items within ULDs to specific belly positions.

The methodology employed in this study is innovative, integrating the APP and WBP in a way not previously addressed in the literature. The process begins with input data on cargo items, PAX, BAX, aircraft, and fuel. Initially, the model solves a 1D-BPP combined with a WBP, 1D-BPP-W&B, determining the optimal configuration of items within ULDs and their respective positions in the aircraft's belly hold, respecting safety and CG envelope constraints using a MILP formulation. Subsequently, the model utilizes a 3D-BPP heuristic to attempt packing cargo items within their assigned ULDs. If the initial packing configuration fails, a feedback loop is activated, revisiting the 1D-BPP-W&B and 3D-BPP iteratively until a feasible packing solution is achieved for all items.

The effectiveness of the integrated model was assessed through a scenario analysis involving 138 flights. Four scenarios were tested to evaluate model performance. The integrated APP and WBP model determined the optimal placement of cargo items in their corresponding ULDs and belly positions. The sequential scenario simulated traditional operational practices where ULDs are first constructed and later optimized for the aircraft's W&B, providing a benchmark to compare the integrated model. The W&B-focused scenario involved optimizing the aircraft W&B using the ULDs built for the actual flight, demonstrating potential improvements in W&B if the belly configuration was optimized. The actual scenario represented the real-world conditions of the aircraft at takeoff, including the actual loading and belly configuration, and provided an understanding of the current operational practices compared to the proposed integrated model.

The integrated model showed the highest fuel efficiency improvements across all scenarios, with an average saving of 0.53% per flight. The sequential scenario performed relatively well compared to the actual and W&B-focused scenarios, primarily because it employed the fewest ULDs. This efficient build of ULDs reduced the total number of ULDs and expanded the available solution space for strategically positioning ULDs towards the aircraft's rear compartments, thereby optimizing the %MAC at ZFW by reducing the number of ULDs in the front compartment. Although the W&B-focused scenario did not perform as well as the integrated model, it still showed potential for future research and application for the Load Control department of our partner airline.

While the integrated model has demonstrated significant benefits in improving fuel efficiency, its real-world application may encounter several operational challenges. One significant challenge lies in the transition and training required for warehouse personnel to adapt to building ULDs according to the model's output, as it is a crucial part of maintaining the integrity of the model's recommendations. Additionally, the adaptation of the model configurations by load controllers presents another critical challenge. Load controllers often prioritize operational efficiencies at the departure and arrival airports, focusing on accelerating the loading and unloading processes. This practice might deviate from the model's optimized belly configurations, potentially compromising the aircraft's W&B designed to enhance fuel efficiency.

Given these considerations, future research should investigate the practicalities of implementing this model under real-world conditions. This includes exploring cargo availability dynamics and aligning ground operations with the model outputs under time constraints. The most considerable accomplishment would be to refine the model integration into live operations, ensuring it can respond dynamically to the operational environment and continue to offer considerable fuel savings.

Moving forward, the potential transition of the integrated model to real-time operations represents a significant advancement in air cargo logistics. The implementation of the integrated APP and WBP in real-time could revolutionize airlines' operational activities, leading to more sustainable practices. Finally, this integrated model paves the way for a greener future in aviation by enhancing operational efficiency and reducing fuel consumption.

References

All Nippon Airways Cargo (2024). Belly position of the boeing 787-10. `https://www.anacargo.jp/en/int/specification/b787_10.html`.

Brandt, F. and Nickel, S. (2019). The air cargo load planning problem - a consolidated problem definition and literature review on related problems. *European Journal of Operational Research*, 275(2):399–410.

Federal Aviation Administration (2016). *Weight and Balance Handbook*. United States Departement of Transportation.

Jozefowska, J., Pawlak, G., Pesch, E., Morze, M., and Kowalski, D. (2018). Fast truck-packing of 3d boxes. *Engineering Management in Production and Services*, 10:29–40.

Limbourg, S., Schyns, M., and Laporte, G. (2012). Automatic aircraft cargo load planning. *Journal of the Operational Research Society*, 63:1271–1283.

Lu, Y., Dong, C., Nan, M., Chen, X., and Wei, Y. (2023). Optimal method of air cargo loading under multi-constraint conditions. In Wang, Y., Liu, Y., Zou, J., and Huo, M., editors, *Signal and Information Processing, Networking and Computers*, pages 300–308, Singapore. Springer Nature Singapore.

Paquay, C., Limbourg, S., Schyns, M., and Oliveira, J. (2018). MIP-based constructive heuristics for the three-dimensional Bin Packing Problem with transportation constraints. *International Journal of Production Research*, 56(4):1581–1592.

Paquay, C., Schyns, M., and Limbourg, S. (2014). A mixed integer programming formulation for the three-dimensional bin packing problem deriving from an air cargo application. *International Transactions in Operational Research*, 23(1-2):187–213.

Reick, B. (2021). Basic analysis of bin-packing heuristics. *ArXiv*, abs/2104.12235.

Silva, E. F., Toffolo, T. A. M., and Wauters, T. (2019). Exact methods for three-dimensional cutting and packing: A comparative study concerning single container problems. *Computers and Operations Research*, 109:12–27.

Vancroonenburg, W., Verstichel, J., Tavernier, K., and Vanden Berghe, G. (2014). Automatic air cargo selection and weight balancing: A mixed integer programming approach. *Transportation Research Part E: Logistics and Transportation Review*, 65:70–83.

Zhao, X., Yuan, Y., Dong, Y., and Zhao, R. (2021). Optimization approach to the aircraft weight and balance problem with the centre of gravity envelope constraints. *IET Intelligent Transport Systems*, 15:18.

Appendices

A 1D Bin Packing & Weight and Balance Problem

A.1 Mathematical Formulation

Table 1: Sets for the 1D Bin Packing & Weight and Balance Problem.

Set	Description
$\mathcal{A}$	set of aircraft types, indexed by a
$\mathcal{G}$	set of flights, indexed by g
$\mathcal{I}_g$	set of items of flight g , indexed by i
$\mathcal{COL}$	subset of items $\mathcal{I}_g$ that need cooling storage
$\mathcal{CRT}$	subset of items $\mathcal{I}_g$ that need controlled room temperature storage
$\mathcal{U}_g$	set of ULDs of flight g, indexed by j
$\mathcal{N}$	subset of BAX, BUP and T ULDs of $\mathcal{U}_g$
$\mathcal{BAX}$	subset of BAX ULDs of $\mathcal{U}_g$
$\mathcal{P}_a$	set of available positions for aircraft type a, indexed by t
$\mathcal{P}_{a,j}$	set of available positions in aircraft type a for ULD j
$\mathcal{P}_{a,left}$	set of available left-sided positions in aircraft type a
$\mathcal{P}_{a,right}$	set of available right-sided positions in aircraft type a
$\mathcal{K}_a$	set of available belly compartments in aircraft type a, indexed by k
$\mathcal{K}_{a,front}$	set of available forward belly compartments in aircraft type a
$\mathcal{K}_{a,aft}$	set of available aft belly compartments in aircraft type a
$\mathcal{P}_{a,k}$	set of available positions in aircraft type a for belly compartment k
$\mathcal{O}_{a,t}$	set of overlapping positions in aircraft type a for position t
$\mathcal{E}_g$	set of payload weights of flight g, indexed by e, consisting of TOW_g, LW_g and ZFW_g

Table 2: Parameters for the 1D Bin Packing & Weight and Balance Problem.

Parameter	Description
m_i	weight of item i
v_i	volume of item i
b_i	booking number of item i
WC_j	weight capacity of ULD j
W_j	weight of ULD j
VC_j	volume capacity of ULD j
$Type_j$	type of ULD j
VT	volume threshold of items in AKE ULDs
$M_{a,t}$	maximum weight in aircraft type a for position t
$d_{a,t}$	distance in aircraft type a from position t to a cargo door
$M_{a,k}$	maximum weight in aircraft type a for belly compartment k
TOW_g	takeoff weight of flight g
LW_g	landing weight of flight g
ZFW_g	zero fuel weight of flight g
$INDEX_{a,PAX,g}$	index for aircraft type a of the passenger aboard flight g
$INDEX_{a,FWD,e}$	forward index limit of aircraft type a at payload weight e
$INDEX_{a,AFT,e}$	aft index limit of aircraft type a at payload weight e
$\Delta INDEX_{a,k}$	delta index of aircraft type a for belly compartment k

Table 3: Decision variables for the 1D Bin Packing & Weight and Balance Problem.

Decision Variable	Type	Description
f_{jt}	binary	equals 1 if ULD j is assigned to position t, 0 otherwise
u_j	binary	equals 1 if ULD j is active, 0 otherwise
p_{ij}	binary	equals 1 if item i is assigned to ULD j, 0 otherwise
SP_{b_i}	binary	equals 1 if any item with the same booking number b_i is not assigned to the same ULD j, 0 otherwise
w_{ijt}	continuous	weight of item i assigned to ULD j at position t

The MILP formulation of the 1D Bin Packing & Weight and Balance Problem is as follows:

$$\max \quad \%MAC_{ZFW} \tag{2}$$

$$\min \quad \sum_{j\in\mathcal{U}_g}\left(\sum_{i\in\mathcal{I}_g,Type_j=\text{AKE}} p_{ij}*(VT-v_i)+\sum_{i\in\mathcal{I}_g,Type_j\neq\text{AKE}} p_{ij}*(VT-v_i)\right) \tag{3}$$

$$\min \quad \sum_{j\in\mathcal{U}_g} u_j \tag{4}$$

$$\min \quad \sum_{j\in\mathcal{U}_g}\left(0.2-\frac{\sum_{i\in\mathcal{I}_g}(v_i*p_{ij})}{VC_j}\right) \tag{5}$$

$$\min \quad \sum_{j\in\mathcal{U}_g}\left(\sum_{i\in\mathcal{I}_g} SP_{b_i}\right) \tag{6}$$

$$\min \quad \sum_{j\in\mathcal{BAX}}\sum_{t\in\mathcal{P}_a} d_{a,t}*f_{jt} \tag{7}$$

s.t.:

$$\sum_{i\in\mathcal{I}_g} m_i p_{ij} \leq WC_j * u_j \qquad \forall j\in\mathcal{U}_g \tag{8}$$

$$\sum_{i\in\mathcal{I}_g} v_i p_{ij} \leq VC_j * u_j \qquad \forall j\in\mathcal{U}_g \tag{9}$$

$$\sum_{j\in\mathcal{U}_g} p_{ij} = 1 \qquad \forall i\in\mathcal{I}_g \tag{10}$$

$$p_{ij} = 0 \qquad \forall i\in\mathcal{I}_g, \forall j\in\mathcal{N} \tag{11}$$

$$\sum_{t\in\mathcal{P}_a} f_{jt} = u_j \qquad \forall j\in\mathcal{U}_g \tag{12}$$

$$\sum_{t\in\mathcal{P}_a} f_{jt} \leq 1 \qquad \forall j\in\mathcal{U}_g \tag{13}$$

$$\sum_{t\notin\mathcal{P}_{a,j}} f_{jt} = 0 \qquad \forall j\in\mathcal{U}_g \tag{14}$$

$$\sum_{t\in\mathcal{P}_a} f_{jt} = 1 \qquad \forall j\in\mathcal{N} \tag{15}$$

$$f_{j_1t_1}+f_{j_2t_2}\leq 1 \qquad \forall j_1,j_2\in\mathcal{U}_g, j_1\neq j_2, t_1\in\mathcal{P}_a, t_2\in\mathcal{O}_{a,t_1} \tag{16}$$

$$w_{ijt}\leq M*p_{ij} \qquad \forall i\in\mathcal{I}_g,\forall j\in\mathcal{U}_g,\forall t\in\mathcal{P}_a \tag{17}$$

$$w_{ijt}\leq M*f_{jt} \qquad \forall i\in\mathcal{I}_g,\forall j\in\mathcal{U}_g,\forall t\in\mathcal{P}_a \tag{18}$$

$$w_{ijt}\geq m_i-M(1-p_{ij}f_{jt}) \qquad \forall i\in\mathcal{I}_g,\forall j\in\mathcal{U}_g,\forall t\in\mathcal{P}_a \tag{19}$$

$$w_{ijt}\leq m_i \qquad \forall i\in\mathcal{I}_g,\forall j\in\mathcal{U}_g,\forall t\in\mathcal{P}_a \tag{20}$$

$$\sum_{i\in\mathcal{I}_g}\sum_{j\in\mathcal{U}_g} w_{ijt}+\sum_{j\in\mathcal{N}} W_j f_{jt}\leq M_{a,t} \qquad \forall t\in\mathcal{P}_a \tag{21}$$

$$\sum_{i\in\mathcal{I}_g}\sum_{j\in\mathcal{U}_g} w_{ijt}+\sum_{j\in\mathcal{N}} W_j f_{jt}\leq M_{a,k} \qquad \forall k\in\mathcal{K}_a,\forall t\in\mathcal{P}_{a,k} \tag{22}$$

$$\sum_{i\in\mathcal{I}_g}\sum_{j\in\mathcal{U}_g} w_{ijt}+\sum_{j\in\mathcal{N}} W_j f_{jt}\leq M_{a,k} \qquad \forall k\in\mathcal{K}_{a,front},\forall t\in\mathcal{P}_{a,k} \tag{23}$$

$$\sum_{i\in\mathcal{I}_g}\sum_{j\in\mathcal{U}_g} w_{ijt}+\sum_{j\in\mathcal{N}} W_j f_{jt}\leq M_{a,k} \qquad \forall k\in\mathcal{K}_{a,rear},\forall t\in\mathcal{P}_{a,k} \tag{24}$$

$$\left|\left(\sum_{t_{left}\in\mathcal{P}_{a,left}}\sum_{j_1\in\mathcal{U}_g}\sum_{i\in\mathcal{I}_g} w_{ij_1t_{left}}+\sum_{t_{left}\in\mathcal{P}_{a,left}}\sum_{j_1\in\mathcal{N}} W_{j_1}f_{j_1t_{left}}\right)-\right.$$
$$\left.\left(\sum_{t_{right}\in\mathcal{P}_{a,right}}\sum_{j_2\in\mathcal{U}_g}\sum_{i\in\mathcal{I}_g} w_{ij_2t_{right}}+\sum_{t_{right}\in\mathcal{P}_{a,right}}\sum_{j_2\in\mathcal{N}} W_{j_2}f_{j_2t_{right}}\right)\right|\leq$$

$$a_{LatTOW} * \left(\sum_{t \in \mathcal{P}_a} \sum_{i \in \mathcal{I}_g} \sum_{j \in \mathcal{U}_g} w_{ijt} + \sum_{t \in \mathcal{P}_a} \sum_{j \in \mathcal{N}} W_j f_{jt} + OEW + TOF \right) + b_{LatTOW} \tag{25}$$

$$\left| \left(\sum_{t_{left} \in \mathcal{P}_{a,left}} \sum_{j_1 \in \mathcal{U}_g} \sum_{i \in \mathcal{I}_g} w_{ij_1 t_{left}} + \sum_{t_{left} \in \mathcal{P}_{a,left}} \sum_{j_1 \in \mathcal{N}} W_{j_1} f_{j_1 t_{left}} \right) - \left(\sum_{t_{right} \in \mathcal{P}_{a,right}} \sum_{j_2 \in \mathcal{U}_g} \sum_{i \in \mathcal{I}_g} w_{ij_2 t_{right}} + \sum_{t_{right} \in \mathcal{P}_{a,right}} \sum_{j_2 \in \mathcal{N}} W_{j_2} f_{j_2 t_{right}} \right) \right| \leq$$

$$a_{LatLW} * \left(\sum_{t \in \mathcal{P}_a} \sum_{i \in \mathcal{I}_g} \sum_{j \in \mathcal{U}_g} w_{ijt} + \sum_{t \in \mathcal{P}_a} \sum_{j \in \mathcal{N}} W_j f_{jt} + OEW + TOF - TripFuel \right) + b_{LatLW} \tag{26}$$

$$INDEX_{a,FWD,e} \leq DOI + FI + INDEX_{a,PAX,g} + \sum_{k \in \mathcal{K}_a} \left(\sum_{i \in \mathcal{I}_g} \sum_{j \in \mathcal{U}_g} \sum_{t \in \mathcal{P}_{a,k}} w_{ijt} + \sum_{j \in \mathcal{N}} \sum_{t \in \mathcal{P}_{a,k}} W_j f_{jt} \right) * \Delta INDEX_{a,k} \tag{27}$$

$\forall e \in \mathcal{E}_g$

$$DOI + FI + INDEX_{a,PAX,g} + \sum_{k \in \mathcal{K}_a} \left(\sum_{i \in \mathcal{I}_g} \sum_{j \in \mathcal{U}_g} \sum_{t \in \mathcal{P}_{a,k}} w_{ijt} + \sum_{j \in \mathcal{N}} \sum_{t \in \mathcal{P}_{a,k}} W_j f_{jt} \right) * \Delta INDEX_{a,k} \leq INDEX_{a,AFT,e} \tag{28}$$

$\forall e \in \mathcal{E}_g$

$$p_{i_1 j} + p_{i_2 j} \leq 1 \qquad \forall i_1 \in \mathcal{COL}, i_2 \in \mathcal{CRT}, j \in \mathcal{U}_g \tag{29}$$

Special handling constraints for aircraft types Boeing 777-200ER and 777-300ER

$$COL_{front} \leq p_{ij} \qquad \forall i \in \mathcal{COL}, j \in \mathcal{U}_g \tag{30}$$
$$COL_{front} \leq f_{jt} \qquad \forall j \in \mathcal{U}_g, t \in \mathcal{K}_{a,front} \tag{31}$$
$$COL_{front} \geq p_{ij} + f_{jt} - 1 \qquad \forall i \in \mathcal{CRT}, j \in \mathcal{U}_g, t \in \mathcal{K}_{a,front} \tag{32}$$
$$CRT_{front} \leq p_{ij} \qquad \forall i \in \mathcal{CRT}, j \in \mathcal{U}_g \tag{33}$$
$$CRT_{front} \leq f_{jt} \qquad \forall j \in \mathcal{U}_g, t \in \mathcal{K}_{a,front} \tag{34}$$
$$CRT_{front} \geq p_{ij} + f_{jt} - 1 \qquad \forall i \in \mathcal{CRT}, j \in \mathcal{U}_g, t \in \mathcal{K}_{a,front} \tag{35}$$
$$\sum_{t \in \mathcal{K}_{a,front}} COL_{front} + CRT_{front} = 0 \tag{36}$$
$$COL_{rear} \leq p_{ij} \qquad \forall i \in \mathcal{COL}, j \in \mathcal{U}_g \tag{37}$$
$$COL_{rear} \leq f_{jt} \qquad \forall j \in \mathcal{U}_g, t \in \mathcal{K}_{a,rear} \tag{38}$$
$$COL_{rear} \geq p_{ij} + f_{jt} - 1 \qquad \forall i \in \mathcal{CRT}, j \in \mathcal{U}_g, t \in \mathcal{K}_{a,rear} \tag{39}$$
$$CRT_{rear} \leq p_{ij} \qquad \forall i \in \mathcal{CRT}, j \in \mathcal{U}_g \tag{40}$$
$$CRT_{rear} \leq f_{jt} \qquad \forall j \in \mathcal{U}_g, t \in \mathcal{K}_{a,rear} \tag{41}$$
$$CRT_{rear} \geq p_{ij} + f_{jt} - 1 \qquad \forall i \in \mathcal{CRT}, j \in \mathcal{U}_g, t \in \mathcal{K}_{a,rear} \tag{42}$$
$$\sum_{t \in \mathcal{K}_{a,rear}} COL_{rear} + CRT_{rear} = 0 \tag{43}$$

Special handling constraints for aircraft types Boeing 787-9 and 787-10

$$COLandCRT_{rear} \leq p_{ij} \qquad \forall i \in \mathcal{COL} \cup \mathcal{CRT}, j \in \mathcal{U}_g \tag{44}$$
$$COLandCRT_{rear} \leq f_{jt} \qquad \forall j \in \mathcal{U}_g, t \in \mathcal{K}_{a,rear} \tag{45}$$
$$COLandCRT_{rear} \geq p_{ij} + f_{jt} - 1 \qquad \forall i \in \mathcal{COL} \cup \mathcal{CRT}, j \in \mathcal{U}_g, t \in \mathcal{K}_{a,rear} \tag{46}$$
$$\sum_{t \in \mathcal{K}_{a,rear}} COLandCRT_{rear} = 0 \tag{47}$$

A.2 Linearized Constraints

Linearization of constraint 19

Table 4: Decision variables for the linearization of constraint 19.

Decision Variable	Type	Description
z_{ijt}	binary	equals 1 if item i assigned to ULD j at position t, 0 otherwise

$$z_{ijt} \leq p_{ij} \qquad \forall i \in \mathcal{I}_g, \forall j \in \mathcal{U}_g, \forall t \in \mathcal{P}_a \tag{48}$$
$$z_{ijt} \leq f_{jt} \qquad \forall i \in \mathcal{I}_g, \forall j \in \mathcal{U}_g, \forall t \in \mathcal{P}_a \tag{49}$$
$$z_{ijt} \geq p_{ij} + f_{jt} - 1 \qquad \forall i \in \mathcal{I}_g, \forall j \in \mathcal{U}_g, \forall t \in \mathcal{P}_a \tag{50}$$
$$w_{ijt} \leq m_i - M(1 - z_{ijt}) \qquad \forall i \in \mathcal{I}_g, \forall j \in \mathcal{U}_g, \forall t \in \mathcal{P}_a \tag{51}$$

Linearization of constraints 25 and 26

$$\left(\sum_{t_{left} \in \mathcal{P}_{a,left}} \sum_{j_1 \in \mathcal{U}_g} \sum_{i \in \mathcal{I}_g} w_{ij_1 t_{left}} + \sum_{t_{left} \in \mathcal{P}_{a,left}} \sum_{j_1 \in \mathcal{N}} W_{j_1} f_{j_1 t_{left}} \right) -$$
$$\left(\sum_{t_{right} \in \mathcal{P}_{a,right}} \sum_{j_2 \in \mathcal{U}_g} \sum_{i \in \mathcal{I}_g} w_{ij_2 t_{right}} + \sum_{t_{right} \in \mathcal{P}_{a,right}} \sum_{j_2 \in \mathcal{N}} W_{j_2} f_{j_2 t_{right}} \right) \leq$$
$$a_{LatTOW} * \left(\sum_{t \in \mathcal{P}_a} \sum_{i \in \mathcal{I}_g} \sum_{j \in \mathcal{U}_g} w_{ijt} + \sum_{t \in \mathcal{P}_a} \sum_{j \in \mathcal{N}} W_j f_{jt} + OEW + TOF \right) + b_{LatTOW} \tag{52}$$
$$\left(\sum_{t_{right} \in \mathcal{P}_{a,right}} \sum_{j_2 \in \mathcal{U}_g} \sum_{i \in \mathcal{I}_g} w_{ij_2 t_{right}} + \sum_{t_{right} \in \mathcal{P}_{a,right}} \sum_{j_2 \in \mathcal{N}} W_{j_2} f_{j_2 t_{right}} \right) -$$
$$\left(\sum_{t_{left} \in \mathcal{P}_{a,left}} \sum_{j_1 \in \mathcal{U}_g} \sum_{i \in \mathcal{I}_g} w_{ij_1 t_{left}} + \sum_{t_{left} \in \mathcal{P}_{a,left}} \sum_{j_1 \in \mathcal{N}} W_{j_1} f_{j_1 t_{left}} \right) \leq$$
$$a_{LatTOW} * \left(\sum_{t \in \mathcal{P}_a} \sum_{i \in \mathcal{I}_g} \sum_{j \in \mathcal{U}_g} w_{ijt} + \sum_{t \in \mathcal{P}_a} \sum_{j \in \mathcal{N}} W_j f_{jt} + OEW + TOF \right) + b_{LatTOW} \tag{53}$$
$$\left(\sum_{t_{left} \in \mathcal{P}_{a,left}} \sum_{j_1 \in \mathcal{U}_g} \sum_{i \in \mathcal{I}_g} w_{ij_1 t_{left}} + \sum_{t_{left} \in \mathcal{P}_{a,left}} \sum_{j_1 \in \mathcal{N}} W_{j_1} f_{j_1 t_{left}} \right) -$$
$$\left(\sum_{t_{right} \in \mathcal{P}_{a,right}} \sum_{j_2 \in \mathcal{U}_g} \sum_{i \in \mathcal{I}_g} w_{ij_2 t_{right}} + \sum_{t_{right} \in \mathcal{P}_{a,right}} \sum_{j_2 \in \mathcal{N}} W_{j_2} f_{j_2 t_{right}} \right) \leq$$
$$a_{LatLW} * \left(\sum_{t \in \mathcal{P}_a} \sum_{i \in \mathcal{I}_g} \sum_{j \in \mathcal{U}_g} w_{ijt} + \sum_{t \in \mathcal{P}_a} \sum_{j \in \mathcal{N}} W_j f_{jt} + OEW + TOF - TripFuel \right) + b_{LatLW} \tag{54}$$
$$\left(\sum_{t_{right} \in \mathcal{P}_{a,right}} \sum_{j_2 \in \mathcal{U}_g} \sum_{i \in \mathcal{I}_g} w_{ij_2 t_{right}} + \sum_{t_{right} \in \mathcal{P}_{a,right}} \sum_{j_2 \in \mathcal{N}} W_{j_2} f_{j_2 t_{right}} \right) -$$
$$\left(\sum_{t_{left} \in \mathcal{P}_{a,left}} \sum_{j_1 \in \mathcal{U}_g} \sum_{i \in \mathcal{I}_g} w_{ij_1 t_{left}} + \sum_{t_{left} \in \mathcal{P}_{a,left}} \sum_{j_1 \in \mathcal{N}} W_{j_1} f_{j_1 t_{left}} \right) \leq$$
$$a_{LatLW} * \left(\sum_{t \in \mathcal{P}_a} \sum_{i \in \mathcal{I}_g} \sum_{j \in \mathcal{U}_g} w_{ijt} + \sum_{t \in \mathcal{P}_a} \sum_{j \in \mathcal{N}} W_j f_{jt} + OEW + TOF - TripFuel \right) + b_{LatLW} \tag{55}$$

B 3D Bin Packing Problem Algorithms

B.1 Determine the Following Item and its Placement

Algorithm 1 Find the best next item to place and its placement in the ULD using the merit function

Inputs:

- Set of cargo items **I** with dimensions length l_i, width w_i and height h_i and special handling constraint stackable $stack_i$ equals to 0 if stackable otherwise equals to 1 to be placed in ULD j
- Set of Extreme Points **EP** with coordinates (x_{ep}, y_{ep}, z_{ep}) in ULD j
- PlacedItems: Dictionary of placed items in ULD j with coordinates (x_i, y_i, z_i) and dimensions l_i, w_i and h_i

Functions:

- GetOrientation(item): function returning all possible orientations of item i, see Algorithm 2
- DoesItemFitUld(ep, orientation, j): function returning **true** if item i fits in ULD j at EP ep with orientation **orientation** and **false** otherwise
- CalculateResidualSpace(ep, PlacedItems, j): function returning the residual space around EP ep in ULD j taking into account the items i placed in ULD j per component RS_{left}, RS_{right}, RS_{front}, RS_{back} and RS_{top}
- CheckCollision(ep, length, width, height, PlacedItems, stack): function returning **true** if the item i collides with other items in ULD j at EP ep and **false** otherwise
- IsFullySupported(ep, orientation, PlacedItems, j): function returning **true** if the item i is fully supported by other items in ULD j, ULD j sides and if item i has a stable base at EP ep with orientation **orientation** and **false** otherwise

```
BestOverallMerit ← ∞
BestItemForPlacement ← None
BestPlacementDetails ← None, consisting of a tuple of the best EP, orientation, merit, and support count of the item
Separate Stackables and non-stackables into two lists of cargo items
for PriortizedGroup in [Stackables, Non-stackables] do
  for i in PriortizedGroup do
    BestItemMerit ← ∞
    BestEpItem ← None
    BestOrientationItem ← None
    BestSupportCount ← ∞
    Separate Ground EPs and non-ground EPs into two lists of EPs
    for ep in Ground EPs do
      for orientation in GetOrientation(i) do
        if DoesItemFitUld(ep, orientation, j) then
          ResidualSpace = CalculateResidualSpace(ep, PlacedItems, j)
          if CheckCollision(ep, length, width, height, PlacedItems, stack) then
            continue
          end if
          stable, support-count = IsFullySupported(ep, orientation, PlacedItems, j)
          if not stable then
            continue
          end if
```

Merit = (max($RS_{left} - l_i$, 0) + max($RS_{right} - l_i$, 0) +
max($RS_{front} - w_i$, 0) + max($RS_{back} - w_i$, 0) +
max($RS_{top} - h_i$, 0))
if Merit < BestItemMerit **or**
(Merit == BestItemMerit **and** SupportCount > BestSupportCount) **then**
BestItemMerit = Merit
BestEpItem = ep
BestOrientationItem = orientation
BestSupportCount = SupportCount
end if
end if
end for
end for
if BestItemMerit = ∞ **then**
Redo the process for non-ground EPs
end if
if BestItemMerit < BestOverallMerit **then**
BestOverallMerit = BestItemMerit
BestItemForPlacement = i
BestPlacementDetails = (BestEpItem, BestOrientationItem, BestItemMerit, BestSupportCount)
end if
end for
end for
Output BestItemForPlacement, BestPlacementDetails

B.2 Item Orientation Algorithm

Algorithm 2 Get Item Orientation Possibilities

Input item i with dimensions length l_i, width w_i and height h_i and special handling constraint rotatable $rotatable_i$
if $rotatble_i$ is **false then**
Orientation = $[(l_i, w_i, h_i])$
else
Orientation = $[(l_i, w_i, h_i)$, (l_i, h_i, w_i), (w_i, l_i, h_i), (w_i, h_i, l_i), (h_i, l_i, w_i), $(h_i, w_i, l_i)]$
end if
Output Orientation

B.3 Extreme Points Heuristics Algorithm with a Merit Function

Algorithm 3 Extreme Points Heuristic with merit function

Inputs:

- Results1DBPPWB: Dictionary containing the 1D packing results for each ULD j with the items i assigned to it from the 1D-BPP-W&B block

Functions:

- GetStartingEPs(j): function returning the starting EPs for ULD j
- FindBestNextItemandPlacement(ItemsToPlace, j, PlacedItems, EPs): function returning the best next item to place and its placement in ULD j using the merit function algorithm, described in Algorithm 1
- PlaceItem(item, ep, PlacedItems, orientation, EPs): function placing the item i at EP ep with orientation in ULD j and updating the PlacedItems dictionary
- UpdateExtremePoints(EPs, PlacedItems, item, j): function updating the global list of EPs after placing item i at EP ep with orientation in ULD j

```
DeferredItems ← ∅
AllPlacedItems ← ∅
AllEPs ← ∅
for j, items in Results1DBPPWB do
    EPs = GetStartingEPs(j)
    ItemsToPlace = items
    PlacedItems ← ∅
    List of DeferredItems for ULD j ← ∅
    while ItemsToPlace not empty do
        next-item, (ep, orientation, merit, support-count) = FindBestNextItemandPlacement(ItemsToPlace, j,
        PlacedItems, EPs)
        if next-item then
            PlacedItems, = PlaceItem(next-item, ep, PlacedItems, orientation, EPs)
            EPs = UpdateExtremePoints(EPs, PlacedItems, next-item, j)
            ItemsToPlace remove next-item
        else
            DeferredItems for ULD j append next-item
            ItemsToPlace ← ∅
        end if
    end while
    AllPlacedItems for ULD j = PlacedItems
    AllEPs for ULD j = EPs
end for
Output DeferredItems, AllPlacedItems, AllEPs
```

C ULD Type Specifications

PMC

Type: Pallet
Length x Width x Height: 318 x 244 x 162 cm
Maximum Weight: 5102 kg

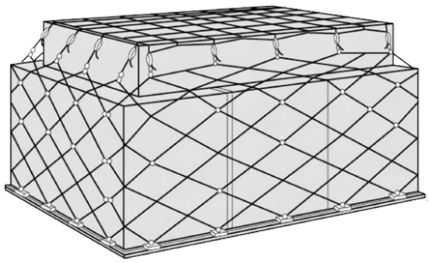

Figure 17: PMC

PAG

Type: Pallet
Length x Width x Height: 318 x 244 x 162 cm
Maximum Weight: 4676 kg

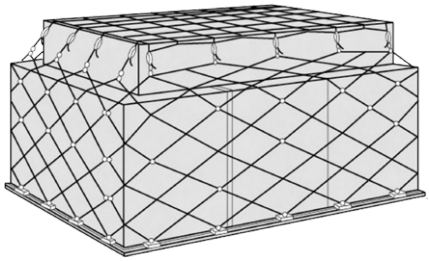

Figure 18: PAG

AKE

Type: Container
Length x Width x Height: 156 x 153 x 162 cm
Maximum Weight: 1587 kg

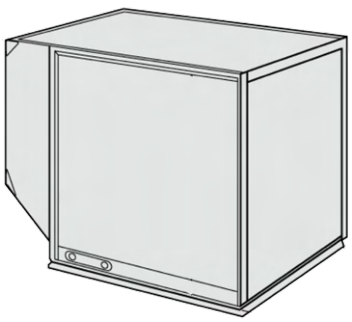

Figure 19: AKE